Enseign. Math. (2) 69 (2023), 93–148
DOI 10.4171/LEM/1049

Spectral triples and ζ-cycles

Alain Connes and Caterina Consani

Abstract. We exhibit very small eigenvalues of the quadratic form associated to the Weil explicit formulas restricted to test functions whose support is within a fixed interval with upper bound S. We show both numerically and conceptually that the associated eigenvectors are obtained by a simple arithmetic operation of finite sum using prolate spheroidal wave functions associated to the scale S. Then we use these functions to condition the canonical spectral triple of the circle of length $L = 2\log(S)$ in such a way that they belong to the kernel of the perturbed Dirac operator. We give numerical evidence that, when one varies L, the low lying spectrum of the perturbed spectral triple resembles the low lying zeros of the Riemann zeta function. We justify conceptually this result and show that, for each eigenvalue, the coincidence is perfect for the special values of the length L of the circle for which the two natural ways of realizing the perturbation give the same eigenvalue. This fact is tested numerically by reproducing the first thirty one zeros of the Riemann zeta function from our spectral side, and estimate the probability of having obtained this agreement at random, as a very small number whose first fifty decimal places are all zero. The theoretical concept which emerges is that of zeta cycle and our main result establishes its relation with the critical zeros of the Riemann zeta function and with the spectral realization of these zeros obtained by the first author.

Mathematics Subject Classification (2020). Primary 11M55; Secondary 11M06, 46L87, 58B34.

Keywords. Spectral triple, Weil positivity, Riemann zeta function, spectral realization, prolate spheroidal functions.

1. Introduction

When contemplating the low lying zeros of the Riemann zeta function one is tempted to speculate that they may form the spectrum of an operator of the form $\frac{1}{2} + iD$ with $D = D^*$ self-adjoint, and to search for the geometry provided by a spectral triple[1] for which D is the Dirac operator. In this paper we give the construction

[1] A triple $(\mathcal{A}, \mathcal{H}, D)$ where $\mathcal{A}$ is an algebra acting in the Hilbert space $\mathcal{H}$ and D is an unbounded self-adjoint operator in $\mathcal{H}$, this is the basic paradigm of noncommutative geometry [3].

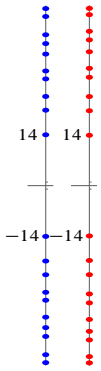

Figure 1
The low lying spectrum of $iD(\lambda, k)$ for $\lambda^2 = 10.5$, $k = 18$, on the left (in blue). On the right (in red), the low lying zeros of the Riemann zeta function.

of a spectral triple $\Theta(\lambda, k) = (\mathcal{A}(\lambda), \mathcal{H}(\lambda), D(\lambda, k))$ which admits, as shown for small values of $\lambda > 1$, a spectrum of $\frac{1}{2} + iD$ very similar to the low lying zeros of the Riemann zeta function (this fact is exemplified in Figure 1, for $\lambda^2 = 10.5$).

More precisely, the spectral triple $\Theta(\lambda, k)$ depends on λ and also on the choice of an integer $k < 2\lambda^2$, moreover for a fixed value of k the positive non-zero eigenvalues $\lambda_n(D(\lambda, k))$ arranged in increasing order, vary continuously with λ. A striking fact (discovered numerically at first) is that for special values of λ the dependence of $\lambda_n(D(\lambda, k))$ on the value of k (close enough to $2\lambda^2$) disappears (see Figure 2 for the case $n = 1$), while the *common value* of these $\lambda_n(D(\lambda, k))$ coincides exactly with the imaginary part of the n-th zero of the Riemann zeta function! This means that the qualitative resemblance of spectra as in Figure 1 yields in fact a sharp coincidence in some range: by varying λ in the interval $5 \leq \lambda^2 \leq 16.5$, and determining the coinciding eigenvalues up to $n = 31$ one produces 31 numbers in amazing agreement with the full collection of values of the first 31 zeros of the zeta function (see Figure 3; incidentally notice that the probability of obtaining such agreement from a random choice is of the order of 10^{-50}).

The main goal of this paper is to provide a theoretical explanation for this numerical "coincidence" and relate it to the spectral realization of the zeros of zeta given in [4]. The new theoretical concept that emerges is that of a ζ-cycle.

In Section 6.1 we explain how to define scale invariant Riemann sums for functions defined on $[0, \infty)$ with vanishing integral. This technique is implemented in the definition of the linear map

$$\Sigma_\mu \mathcal{E} : \mathcal{S}_0^{\mathrm{ev}} \to L^2(C)$$

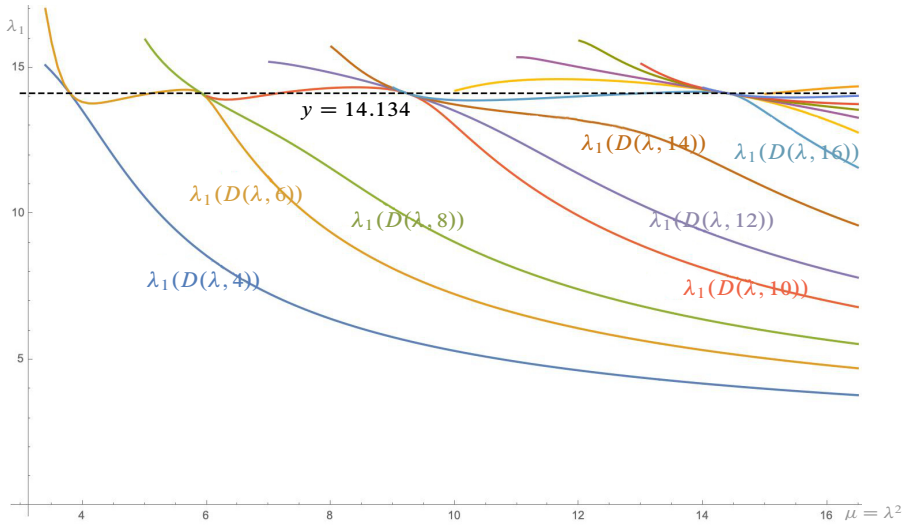

FIGURE 2
The curves represent as a function of $\mu = \lambda^2$ the first positive eigenvalue $\lambda_1(D(\lambda, 2k))$ of $D(\lambda, 2k)$. The ordinate of the points where the graphs touch each other is constant and coincides with the imaginary part $\zeta_1 \sim 14.134$ of the first zero of zeta. The abscissas, i.e. the values of μ, are part of the geometric progression with ratio $\exp(\frac{2\pi}{\zeta_1})$.

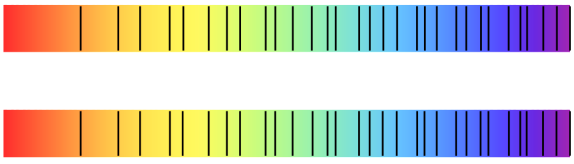

FIGURE 3
Computing the coinciding eigenvalues $\lambda_j(D(\lambda, k))$ one obtains a list (lower line) which one compares with the list (upper line) of imaginary parts ζ_j of zeros of zeta.

from the Schwartz space $\mathcal{S}_0^{\mathrm{ev}}$ of even functions, f, $f(0) = 0$, with vanishing integral, to square integrable functions on the circle $C = \mathbb{R}_+^*/\mu^{\mathbb{Z}}$ of length $L = \log \mu$. The key notion is then provided by the following

Definition 1.1. A *ζ-cycle* is a circle C of length $L = \log \mu$ such that the subspace $\Sigma_\mu \mathcal{E}(\mathcal{S}_0^{\mathrm{ev}})$ is not dense in the Hilbert space $L^2(C)$.

It turns out that likewise for closed geodesics, ζ-cycles are stable under finite covers, and if C is a ζ-cycle of length L, then the n-fold cover of C is a ζ-cycle of length nL, for any positive integer $n > 0$.

By construction, the subspace $\Sigma_\mu \mathcal{E}(\mathcal{S}_0^{\mathrm{ev}}) \subset L^2(C)$ is invariant under the group of rotations of the circle which appears here from the scaling action of the multiplicative group $\mathbb{R}_+^*$ on $C = \mathbb{R}_+^*/\mu^{\mathbb{Z}}$. The main result of this paper is the following

Theorem 1.1. (i) *The spectrum of the action of the multiplicative group $\mathbb{R}_+^*$ on the orthogonal of $\Sigma_\mu \mathcal{E}(\mathcal{S}_0^{\mathrm{ev}})$ in $L^2(C)$ is formed by imaginary parts of zeros of the Riemann zeta function on the critical line.*

(ii) *Let $s > 0$ be such that $\zeta(\frac{1}{2} + is) = 0$, then any circle of length an integral multiple of $2\pi/s$ is a ζ-cycle, and the spectrum of the action of $\mathbb{R}_+^*$ on $(\Sigma_\mu \mathcal{E}(\mathcal{S}_0^{\mathrm{ev}}))^\perp$ contains s.*

The ad-hoc Sobolev spaces used in [4] to provide the spectral realization of zeros of zeta are here replaced by the canonical Hilbert space $L^2(C)$ of square integrable functions. Moreover, Theorem 1.1 provides the theoretical explanation for the above coincidence of spectral values. Indeed, the special values of $\lambda^2 = \mu = \exp L$ at which the k dependence of the eigenvalue $\lambda_n(D(\lambda, k))$ disappear, signal that the related circle of length L is a ζ-cycle and that $\lambda_n(D(\lambda, k))$ is in its spectrum. This explains why the low lying part of the spectrum of the spectral triple $\Theta(\lambda, k)$ possesses a tantalizing resemblance with the low lying zeros of the Riemann zeta function. Indeed, the special values of the length (L) of the circle for which the coinciding $\lambda_n(D(\lambda, k))$ occur, form a part of the arithmetic progression of multiples of $2\pi/\zeta_n$, where ζ_n is the imaginary part of the n-th zero of the zeta function. This forces the graphs of the functions $\lambda_n(D(\mu^{1/2}, k))$ to pass through points of the form $(\exp(2\pi m/\zeta_n), \zeta_n)$ (as in Figure 2) which entails that the low lying spectrum of $D(\lambda, k)$ (for $k \sim 2\lambda^2$) mimics the low lying zeros of the zeta function.

The spectral triple $\Theta(\lambda, k)$ is a finite rank perturbation of the Dirac operator on a circle of length $\log \mu = 2 \log \lambda$ and involves, as a key ingredient, classical prolate spheroidal wave functions [11–13]. These functions are used to define a finite-dimensional subspace (of dimension k) of the Hilbert space of square integrable functions on the circle of length $2 \log \lambda$, and the operator $D(\lambda, k)$ is then *canonically* obtained from the operator of ordinary differentiation $D_0(\lambda)$ to ensure that its kernel contains the above finite-dimensional subspace.

A priori, there seems to be no relation between the construction of the spectral triple $\Theta(\lambda, k)$ and the Riemann zeta function: in Section 3 we explain how we stumbled on $\Theta(\lambda, k)$ while continuing our investigations of the Weil quadratic form restricted to test functions with support in a fixed interval. The Riemann–Weil explicit formulas give a concrete and finite expression of the semi-local Weil quadratic form (see Section 2) which is suitable for numerical exploration since it only involves primes less than, say, λ^2. By semi-local Weil quadratic form we mean the restriction QW_λ of the

sesquilinear form

$$QW(f,g) := \sum_{1/2+is\in Z} \overline{\widehat{f}(\overline{s})}\, \widehat{g}(s) \tag{1.1}$$

on test functions f, g whose support is contained in the interval $[\lambda^{-1}, \lambda] \subset \mathbb{R}^*_+$. In (1.1), Z is the set of non-trivial zeros of the Riemann zeta function and Fourier transform is defined on $C^\infty_c(\mathbb{R}^*_+)$ by

$$\widehat{f}(s) = \mathbb{F}_\mu(f)(s) := \int_{\mathbb{R}^*_+} f(u) u^{-is}\, d^*u. \tag{1.2}$$

One knows that the positivity of the Weil quadratic form QW_λ for all λ implies the Riemann Hypothesis (RH), and in case RH holds, QW_λ is known to be strictly positive. In [14], the positivity was shown to hold for $\lambda = \sqrt{2}$ using numerical analysis. In Section 2 we test numerically this positivity for larger values of λ, showing (Section 2.2) that the contribution from the archimedean place alone ceases to be positive in the upper part of the interval

$$\log(\lambda^2) \in [\log 2 - 0.2, \log 2 + 0.2] \sim [0.493, 0.893],$$

while the positivity is restored by adding the contribution of the prime 2. This latter contribution depends explicitly on $p = 2$ in a form W_p which in fact can be evaluated for any real number $p \sim 2$ (i.e. close to but not equal to 2). We show (Section 2.3) that by requiring positivity one restricts the allowed values of p to an interval of size $\sim 10^{-3}$ around $p = 2$, and in Section 2.4 we display that when λ^2 grows past a prime power and one ignores its contribution, the quadratic form QW_λ fails to remain positive. This fact is displayed up to $\lambda^2 \sim 7$. One striking numerical result is described in Section 2.5, where we report numerical evidence that as λ increases the corresponding operator in $\mathcal{H}(\lambda) := L^2([\lambda^{-1}, \lambda], d^*u)$ admits a finite number of extremely small positive eigenvalues. For instance, we find that when $\lambda^2 = 11$ the smallest positive eigenvalue is 2.389×10^{-48}. The corresponding eigenfunctions are graphically reported in Figures 22, 23, 24.

Section 3 explains conceptually the presence of these extremely small positive eigenvalues and there we also give an excellent approximation of the related eigenfunctions. The theoretical reason for the presence of these extremely small eigenvalues springs from the fact that the radical of the Weil quadratic form contains the range of the map $\mathcal{E}$ of [4], that is defined on the codimension two subspace $\mathcal{S}^{\rm ev}_0$ of even Schwartz functions fulfilling $f(0) = \widehat{f}(0) = 0$ by

$$\mathcal{E}(f)(x) := x^{1/2} \sum_{n>0} f(nx), \quad \forall f \in \mathcal{S}^{\rm ev}_0. \tag{1.3}$$

Even though RH implies that QW_λ is strictly positive, and thus that its radical is $\{0\}$, by making use of (1.3), one can nevertheless construct functions g with support in $[\lambda^{-1},\lambda]$ which are in the "near radical" of the Weil quadratic form, i.e. fulfill $QW_\lambda(g) \ll \|g\|^2$. More precisely, if the support of the even function $f \in \mathcal{S}_0^{\mathrm{ev}}$ is contained in the interval $[-\lambda,\lambda] \subset \mathbb{R}$, the support of $\mathcal{E}(f)$ is contained in $(0,\lambda] \subset \mathbb{R}_+^*$. On the other hand, the Poisson formula

$$\mathcal{E}(\widehat{f})(x) = \mathcal{E}(f)(x^{-1}), \quad \forall f \in \mathcal{S}_0^{\mathrm{ev}} \tag{1.4}$$

shows that the support of $\mathcal{E}(f)$ is contained in $[\lambda^{-1},\infty)$ provided the support of the even function $\widehat{f}$ is contained in the interval $[-\lambda,\lambda] \subset \mathbb{R}$. The obstruction to obtain an element $\mathcal{E}(f)$ of the radical of QW_λ is the equality $\mathcal{P}_\lambda \cap \widehat{\mathcal{P}}_\lambda = \{0\}$, where $\mathcal{P}_\lambda$ and $\widehat{\mathcal{P}}_\lambda$ are the cutoff projections in the Hilbert space $L^2(\mathbb{R})^{\mathrm{ev}}$ of square integrable even functions (the projection $\mathcal{P}_\lambda$ is given by the multiplication by the characteristic function of the interval $[-\lambda,\lambda] \subset \mathbb{R}$, the projection $\widehat{\mathcal{P}}_\lambda$ is its conjugate by the Fourier transform $\mathbb{F}_{e_{\mathbb{R}}}$). The seminal work of Slepian and Pollack [11–13] on band limited functions then shows that while $\mathcal{P}_\lambda \cap \widehat{\mathcal{P}}_\lambda = \{0\}$, the angle operator between these two projections admits a finite number $1 + \nu(\lambda^2) \sim 2\lambda^2$ of extremely small non-zero eigenvalues and that the corresponding eigenfunctions are the prolate spheroidal wave functions

$$\psi_{m,\lambda}(x) := \mathrm{PS}_{2m,0}\Big(2\pi\lambda^2, \frac{x}{\lambda}\Big), \quad m \leq \nu(\lambda^2) \sim 2\lambda^2.$$

By construction, each $\psi_{m,\lambda}$ is a function on the interval $[-\lambda,\lambda]$ that one extends by 0 outside that interval. Its Fourier transform $\mathbb{F}_{e_{\mathbb{R}}}(\psi_{m,\lambda})$ restricted to the interval $[-\lambda,\lambda]$, is equal to $\chi_m\psi_{m,\lambda}$ where the scalar χ_m is very close to $(-1)^m$ provided that m is less than $\nu(\lambda^2) \sim 2\lambda^2$. After taking care of the two conditions $f(0) = \widehat{f}(0) = 0$, the restriction of $\mathcal{E}(f)$ to the interval $[\lambda^{-1},\lambda]$ gives rise to a function which we call a "prolate vector", and on which QW_λ takes non-zero, but extremely small values. This fact is verified concretely in Section 3 where we compare the eigenvectors of the Weil quadratic form QW_λ associated to its smallest eigenvalues with the orthogonalization of the prolate vectors obtained using the technique outlined above, from the prolate spheroidal wave functions.

The construction of the spectral triple $\Theta(\lambda,k)$ is carried out in Section 4. Even though this construction is motivated by the results of Section 3 on the near radical of the Weil quadratic form QW_λ, the technique involved only uses the prolate vectors without any reference to QW_λ. Using the first $k+2$ prolate functions, one obtains a k-dimensional subspace of

$$L^2\big([\lambda^{-1},\lambda], d^*u\big) \simeq L^2\big(\mathbb{R}_+^*/\lambda^{2\mathbb{Z}}, d^*u\big),$$

then one lets $\Pi(\lambda,k)$ be the associated orthogonal projection. By definition, the spectral triple $\Theta(\lambda,k) = (\mathcal{A}(\lambda), \mathcal{H}(\lambda), D(\lambda,k))$ is given by the action by multiplication of the

algebra of smooth functions $\mathcal{A}(\lambda) := C^\infty(\mathbb{R}_+^*/\lambda^{2\mathbb{Z}})$ on $\mathcal{H}(\lambda) := L^2(\mathbb{R}_+^*/\lambda^{2\mathbb{Z}}, d^*u)$, while the operator $D(\lambda, k)$ is the finite rank perturbation

$$D(\lambda,k) := \big(1-\Pi(\lambda,k)\big)\circ D_0 \circ \big(1-\Pi(\lambda,k)\big), \quad D_0 = -iu\partial_u \tag{1.5}$$

of the standard Dirac operator $D_0 = -iu\partial_u$ (with periodic boundary conditions when viewed in $L^2([\lambda^{-1},\lambda], d^*u) \simeq L^2(\mathbb{R}_+^*/\lambda^{2\mathbb{Z}})$). We compute the low lying spectra of these spectral triples and find a neat resemblance with the low lying zeros of the Riemann zeta function, provided that k is sufficiently close to the largest allowed value $\nu(\lambda^2)$. On the other hand, since the eigenvalues $\lambda_n(D(\lambda,k))$ vary with λ, one cannot expect that they reproduce exactly the n-th zero of the zeta function. The subtlety of the relation is explained in Section 5, where we produce several criteria to recover the zeros of the Riemann zeta function using the non-zero eigenvalues $\lambda_n(D(\lambda,k))$. First we show that for $k = 2\ell$, the eigenvalues fulfill the inequality

$$\lambda_n\big(D(\lambda,k+1)\big) \le \lambda_n\big(D(\lambda,k)\big),$$

then we prove (Section 5.1) that for certain values of λ one has

$$\lambda_n\big(D(\lambda,k+1)\big) \simeq \lambda_n\big(D(\lambda,k)\big).$$

When this happens and k is close enough to the upper bound $\nu(\lambda^2)$, the common eigenvalue coincides with the imaginary part of the n-th zero of the zeta function. This result is strengthened in Section 5.2, where we plot the evolution of the eigenvalues $\lambda_n(D(\lambda,k))$, as functions of $\mu = \lambda^2$, for fixed k, and find that several graphs coincide at the above special values of λ as displayed in Figure 2. In Section 5.3 we find that the obtained special points in the (μ, λ_n) plane fulfill the quantization condition

$$\mu^{i\lambda_n} = 1.$$

This result suggests that for the above special values of λ one has an eigenvector which is already an eigenvector of the unperturbed Dirac operator D_0. In Section 5.4 we apply this criterion to select the special values of λ, and compute the first 31 zeros of the Riemann zeta function with the precision shown in Figure 3. The conceptual explanation of these experimental findings is Theorem 1.1 whose proof is developed in the final Section 6.

2. The semi-local Weil quadratic form

In this section we test numerically the positivity of the Weil quadratic form $QW(f,g)$, in the semi-local case, namely for test functions f, g with support in the interval $[\lambda^{-1}, \lambda]$. This investigation breaks down in two independent cases so that

$$QW_\lambda = QW_\lambda^+ \oplus QW_\lambda^-,$$

according to the parity of f and g with respect to the symmetry operator $u \mapsto u^{-1}$.

Lemma 2.5 shows that for real test functions, the even functions do not interfere with the odd ones. Moreover, by construction, the positivity of QW_λ depends on the length $L = 2\log\lambda$ of the support of the test functions. We define in (2.21) an orthonormal basis $\{\eta_n, n \in \mathbb{Z}\}$ of the Hilbert space $L^2([\lambda^{-1}, \lambda])$ formed by odd (for the symmetry $u \mapsto u^{-1}$) real functions for $n < 0$, and by even real functions for $n \geq 0$. The matrix

$$\sigma(n,m) = QW(\eta_n, \eta_m)$$

is the direct sum $\sigma = \sigma^+ \oplus \sigma^-$ of two infinite symmetric real matrices, each of which is expressed as a finite sum involving the archimedean contribution $-W_{\mathbb{R}}$, as well as the contribution $-W_p$ from primes p less than $\mu = \lambda^2$. The numerical tests consist in evaluating the eigenvalues of the very large portion of these matrices corresponding to indices n and m whose absolute values are $\leq N$. These computations give significant evidence that the increasing of large N does not alter substantially the lower part of the spectrum of $\sigma(n,m)$. In Section 2.2 we find that the archimedean contribution $-W_{\mathbb{R}}$ to the Weil quadratic form when taken separately, ends to be positive if computed in an interval extending slightly beyond the value $L = \log 2$ (Figure 6). However, the positivity is restored after that value, and precisely in the interval $\log 2 \leq L < \log 3$, by implementing also the contribution of the prime $p = 2$, in terms of the related functional $-W_2$.

In Section 2.3 we report our numerical findings supplying evidence to the fact that the sign of QW_λ is also sensitive to the replacement of $-W_2$ by a functional $-W_p$ whose definition uses the same formula as $-W_2$ but replaces 2 with p, taken as a real variable in a small neighborhood of $p = 2$. Indeed the computations show that the positivity of the quadratic form fails if one considers real values of p outside an interval of size $< 10^{-3}$ around 2. In Section 2.4 we report graphical evidence indicating how important is the contribution of each functional $-W_p$ to preserve the positivity of the quadratic form, if the support of the test function stretches beyond a prime power p^n. Finally, in Section 2.5 we display numerical evidence of the key fact that by suitably increasing the support of the test functions, the "even" and "odd" matrices $\sigma^\pm$ admit a finite number of extremely small positive eigenvalues. The theoretical discussion of this result is presented in Section 3.

2.1. The matrix $\sigma = \sigma^+ \oplus \sigma^-$. This subsection describes the choice of test functions used in this paper while performing the numerical computations. When viewed in Hilbert theoretic terms the restriction QW_λ of the Weil quadratic form to functions with support in the interval $[\lambda^{-1}, \lambda]$ is a lower bounded, lower semi-continuous quadratic form defined on the Hilbert space $\mathcal{H} := L^2([\lambda^{-1}, \lambda], d^*u)$ with values in $(-\infty, +\infty]$. We choose an orthonormal basis $\{\eta_n\}_{n\in\mathbb{Z}}$ of $\mathcal{H}$ which is a core for QW_λ and compute the eigenvalues of very large portions of the associated matrix $QW(\eta_n, \eta_m) = \sigma(n,m)$.

2.1.1. Explicit formula. Following [2], one considers the class $\mathcal{W}$ of complex valued functions f on $\mathbb{R}_+^*$ which are continuous and with continuous derivative except at finitely many points where both $f(x)$ and $f'(x)$ have at most a discontinuity of the first kind, and at which the value of $f(x)$ and $f'(x)$ is defined as the average of the right and left limits. Moreover, one assumes that for some $\delta > 0$, one has

$$\begin{aligned} f(x) &= O(x^{\delta}) \qquad \text{for } x \to 0+, \\ f(x) &= O(x^{-1-\delta}) \quad \text{for } x \to +\infty. \end{aligned}$$

The Mellin transform of $f \in \mathcal{W}$ is defined as

$$\widetilde{f}(s) := \int_0^\infty f(x) x^{s-1}\, dx. \tag{2.1}$$

Let $f^\sharp(x) := x^{-1} f(x^{-1})$, then Weil's explicit formula takes the form

$$\sum_\rho \widetilde{f}(\rho) = \int_0^\infty f(x)\, dx + \int_0^\infty f^\sharp(x)\, dx - \sum_v \mathcal{W}_v(f), \tag{2.2}$$

where the sum on the left-hand side is over all complex zeros ρ of the Riemann zeta function, and the sum on the right-hand side runs over all rational places v of $\mathbb{Q}$. The non-archimedean distributions $\mathcal{W}_p$ are defined as

$$\mathcal{W}_p(f) := (\log p) \sum_{m=1}^\infty \big(f(p^m) + f^\sharp(p^m)\big), \tag{2.3}$$

while the archimedean distribution is given by

$$\mathcal{W}_{\mathbb{R}}(f) := (\log 4\pi + \gamma) f(1) + \int_1^\infty \Big(f(x) + f^\sharp(x) - \frac{2}{x} f(1)\Big) \frac{dx}{x - x^{-1}}. \tag{2.4}$$

The translation to (equivalent) formulas using the Fourier transform (in place of the Mellin transform) is done by implementing the automorphism Δ

$$f \mapsto \Delta^{1/2} f = F, \quad F(x) = x^{1/2} f(x), \tag{2.5}$$

which respects the convolution product and satisfies the equalities

$$(\Delta^{1/2} f^\sharp)(x) = x^{1/2} f^\sharp(x) = x^{-1/2} f(x^{-1}) = (\Delta^{1/2} f)(x^{-1}).$$

After taking complex conjugates, Δ is compatible with the natural involutions. For a rational place v, we set $W_v(F) := \mathcal{W}_v(\Delta^{-1/2} F)$, then the above distributions $\mathcal{W}_p$ take the following form

$$W_p(F) = (\log p) \sum_{m=1}^\infty p^{-m/2} \big(F(p^m) + F(p^{-m})\big). \tag{2.6}$$

Using the multiplicative version $d^*x = dx/x$ of the Haar measure, the archimedean distribution $\mathcal{W}_{\mathbb{R}}$ becomes

$$W_{\mathbb{R}}(F) := (\log 4\pi + \gamma)F(1) + \int_1^\infty \big(F(x) + F(x^{-1}) - 2x^{-1/2}F(1)\big)\frac{x^{1/2}}{x - x^{-1}}\, d^*x. \tag{2.7}$$

2.1.2. The semi-local Weil quadratic form. The Weil quadratic form is now rewritten as

$$\begin{aligned} QW(f,g) &= \psi(f^* * g), \\ \psi(F) &:= \hat{F}(i/2) + \hat{F}(-i/2) - W_{\mathbb{R}}(F) - \sum_p W_p(F), \end{aligned} \tag{2.8}$$

where

$$\hat{F}(s) := \int F(u)u^{-is}\, d^*u$$

denotes the Fourier transform of the function F. Moreover, the functional $W_\infty := -W_{\mathbb{R}}$ fulfills the following formula

$$W_\infty(F) = \int \hat{F}(t)\frac{2\partial_t\theta(t)}{2\pi}\, dt \tag{2.9}$$

in terms of the derivative of the angular Riemann–Siegel function $\theta(t)$

$$\theta(t) = -\frac{t}{2}\log\pi + \Im\log\Gamma\Big(\frac{1}{4} + i\frac{t}{2}\Big), \tag{2.10}$$

with $\log\Gamma(s)$, for $\Re(s) > 0$, the branch of the log which is real for s real.

By a lower bounded, lower semi-continuous (lsc) quadratic form q on a Hilbert space $\mathcal{H}$ we mean a lower semi-continuous map[2] $q\colon \mathcal{H} \to (-\infty, +\infty]$, which fulfills $q(\lambda\xi) = |\lambda|^2 q(\xi)$ for all $\lambda \in \mathbb{C}$, the parallelogram law

$$q(\xi + \eta) + q(\xi - \eta) = 2q(\xi) + 2q(\eta)$$

and also an inequality of the form $q(\xi) \geq -c\|\xi\|^2$ for all $\xi \in \mathcal{H}$, reflecting the lower bound of q. The associated sesquilinear form (antilinear in the first variable) is given on the domain of q, $\mathrm{Dom}(q) := \{\xi \in \mathcal{H} \mid q(\xi) < \infty\}$ by

$$q(\xi, \eta) := \frac{1}{4}\big(q(\xi + \eta) - q(\xi - \eta) + iq(i\xi + \eta) - iq(i\xi - \eta)\big).$$

[2] i.e. such that when $\xi_n \to \xi$ one has $q(\xi) \leq \liminf q(\xi_n)$.

By a result of Kato (see [10, Theorem 2)]) such lower bounded quadratic forms correspond to lower bounded densely defined self-adjoint operators $T \geq -c$ on $\mathcal{H}$ by the formula

$$q(\xi) + c\|\xi\|^2 = \langle (T+c)^{1/2}\xi \mid (T+c)^{1/2}\xi \rangle = \|(T+c)^{1/2}\xi\|^2, \quad \forall \xi \in \mathcal{H}.$$

At the informal level this means that $q(\xi, \eta) = \langle \xi \mid T\eta \rangle$.

Proposition 2.1. *Let $\lambda > 1$. The following formula defines a lower bounded lower semi-continuous quadratic form $QW_\lambda \colon L^2([\lambda^{-1}, \lambda], d^*u) \to (-\infty, +\infty]$,*

$$QW_\lambda(f,f) := \int |\widehat{f}(t)|^2 \frac{2\partial_t \theta(t)}{2\pi}\, dt + 2\Re\Big(\widehat{f}\Big(\frac{i}{2}\Big)\overline{\widehat{f}}\Big(-\frac{i}{2}\Big)\Big) - \sum_{1<n\leq\lambda^2} \Lambda(n)\langle f \mid V(n) f\rangle, \tag{2.11}$$

where $\Lambda(n)$ is the von Mangoldt function and $V(n)$ is the bounded self-adjoint operator in $L^2([\lambda^{-1}, \lambda], d^*u)$ such that

$$\langle f \mid V(n) g\rangle = n^{-1/2}\big((f^* * g)(n) + (f^* * g)(n^{-1})\big). \tag{2.12}$$

Proof. The function $\partial_t \theta(t)$ is even, lower bounded and of the order of $O(\log|t|)$ for $|t| \to \infty$. This shows that the first term in (2.11),

$$Q_\infty(f) = \int |\widehat{f}(t)|^2 \frac{2\partial_t \theta(t)}{2\pi}\, dt,$$

defines a lower bounded, lower semi-continuous quadratic form Q_∞ on the Hilbert space $L^2(\mathbb{R}_+^*, d^*u)$. We view $L^2([\lambda^{-1}, \lambda], d^*u)$ as the closed subspace of functions which vanish outside $[\lambda^{-1}, \lambda]$. The restriction of the quadratic form Q_∞ to $L^2([\lambda^{-1}, \lambda], d^*u)$ is still lower semi-continuous and lower bounded, moreover the domain

$$\big\{\xi \in L^2\big([\lambda^{-1}, \lambda], d^*u\big) \mid Q_\infty(\xi, \xi) < \infty\big\}$$

is dense since it contains all smooth functions with support in (λ^{-1}, λ). Thus, it remains to show that each of the remaining terms can be written in the form $\langle f \mid Tg\rangle$ with T bounded and self-adjoint in $L^2([\lambda^{-1}, \lambda], d^*u)$. One has

$$\widehat{f}\Big(\frac{i}{2}\Big) = \int_{\lambda^{-1}}^{\lambda} f(u) u^{1/2}\, d^*u = \langle h \mid f\rangle, \quad h(u) := u^{1/2}, \qquad \forall u \in [\lambda^{-1}, \lambda].$$

Thus, the term $2\Re(\widehat{f}(i/2)\overline{\widehat{f}}(-i/2))$ in (2.11) is of the form $\langle f \mid Tf\rangle$, where T is the sum of the rank one operators $T = |h\rangle\langle h^*| + |h^*\rangle\langle h|$. Let us show that (2.12) defines a bounded self-adjoint operator $V(n)$ in $L^2([\lambda^{-1}, \lambda], d^*u)$. One has

$$(f^* * g)(v) = \int f^*(vu^{-1}) g(u)\, d^*u = \int \overline{f(v^{-1}u)} g(u)\, d^*u$$

so that by the Cauchy–Schwarz inequality one derives

$$|(f^* * g)(v)| \leq \|f\|\|g\|.$$

This shows that the equality $(f^* * g)(v) = |f\rangle\langle V_v g|$ defines a bounded operator V_v in $L^2([\lambda^{-1}, \lambda], d^*u)$. Moreover, its adjoint is $V_v^* = V_{v^{-1}}$, and thus $V(n)$ is bounded and self-adjoint. ∎

Lemma 2.2. *Let $\lambda > 1$, and let $U \in L^2([\lambda^{-1}, \lambda], d^*u)$ be the function*

$$U(u) := u^{\frac{i\pi}{\log \lambda}}.$$

Then the space of Laurent polynomials $\mathbb{C}[U, U^{-1}]$ is a core for the quadratic form QW_λ.

Proof. Since all terms in (2.11) are bounded except for Q_∞, it is enough to show that $\mathbb{C}[U, U^{-1}]$ is a core for the quadratic form Q_∞ restricted to $L^2([\lambda^{-1}, \lambda], d^*u)$. First note that the powers U^n belong to the domain of Q_∞ since the Fourier transform of U^n is given by

$$\begin{aligned} \widehat{U^n}(s) &= \int_{\lambda^{-1}}^{\lambda} U^n(u) u^{-is} d^*u = \left[u^{\frac{i\pi n}{\log \lambda} - is} \left(\frac{i\pi n}{\log \lambda} - is \right)^{-1} \right]_{\lambda^{-1}}^{\lambda} \\ &= 2 \log \lambda (-1)^n \sin(s \log \lambda)(\pi n - s \log \lambda)^{-1} = O(1/|s|). \end{aligned} \tag{2.13}$$

Thus, the integral of $|\widehat{U^n}(s)|^2 \partial_t \theta(t)$ is absolutely convergent and U^n belongs to the domain of Q_∞. Next, given $\xi \in L^2([\lambda^{-1}, \lambda], d^*u)$ such that $Q_\infty(\xi, \xi) < \infty$, we want to show that for any $\varepsilon > 0$, there exists $\eta \in \mathbb{C}[U, U^{-1}]$ such that (with $-c$ the lower bound of Q_∞)

$$(1 + c)\|\xi - \eta\|^2 + Q_\infty(\xi - \eta, \xi - \eta) < \varepsilon. \tag{2.14}$$

We switch from $\mathbb{R}_+^*$ to the additive group $\mathbb{R}$ (using the logarithm) and let $L = 2 \log \lambda$ and $\mathcal{H} = L^2([-L/2, L/2]) \subset L^2(\mathbb{R})$. Under this change of variable the function U becomes $U(x) = \exp(2\pi i x/L)$. Moreover, using the Fourier transform on $\mathbb{R} \simeq \widehat{\mathbb{R}}$, one can write

$$Q_\infty(f, f) := \int |\hat{f}(t)|^2 \frac{2\partial_t \theta(t)}{2\pi} \, dt. \tag{2.15}$$

In view of the asymptotic expansion for $|t| \to \infty$,

$$\partial_t \theta(t) = \frac{1}{2}\big(\log(|t|) - \log(2) - \log(\pi)\big) - \frac{1}{48t^2} + O(t^{-4}),$$

one can replace (2.14) by an equivalent condition of finding, given $\varepsilon > 0$, a Laurent polynomial η in $U(x) = \exp(2\pi i x/L)$ for $x \in [-L/2, L/2]$, such that

$$\int |\widehat{\xi}(s) - \widehat{\eta}(s)|^2 \big(1 + \log(1 + s^2)\big)\, ds < \varepsilon. \tag{2.16}$$

We first replace ξ by ξ_1 with $\xi_1(x) := \rho\, \xi(\rho x)$ for $\rho > 1$, while

$$\int |\widehat{\xi}(s) - \widehat{\xi}_1(s)|^2 \big(1 + \log(1 + s^2)\big)\, ds < \varepsilon/2 \tag{2.17}$$

This latter inequality holds provided ρ is close enough to 1. Indeed, one has

$$\int |\widehat{\xi}(s)|^2 \big(1 + \log(1 + s^2)\big)\, ds < \infty, \quad \widehat{\xi}_1(s) = \widehat{\xi}(\rho^{-1} s),$$

while the scaling action S of $\mathbb{R}_+^*$ on the Hilbert space of functions on $\mathbb{R}$ with the norm

$$\|f\|_1^2 := \int |f(s)|^2 \big(1 + \log(1 + s^2)\big)\, ds$$

is pointwise norm continuous. Note first that $S(\rho)$ is bounded uniformly near $\rho = 1$ since

$$\int |f(\rho^{-1} s)|^2 \big(1 + \log(1 + s^2)\big)\, ds = \rho \int |f(t)|^2 \big(1 + \log(1 + \rho^2 t^2)\big)\, dt$$

while

$$\big(1 + \log(1 + \rho^2 t^2)\big) \leq 2\big(1 + \log(1 + t^2)\big)$$

for all $t \in \mathbb{R}$ for $\rho \leq 2$. The pointwise norm continuity of $S(\rho)$ follows since this action is pointwise norm continuous on the dense subspace of continuous functions with compact support. Now the support of ξ_1, $\xi_1(x) := \rho\, \xi(\rho x)$ is contained in the interval $[-\rho^{-1} L/2, \rho^{-1} L/2]$. Thus, the convolution $\xi_2 = \phi * \xi_1$ with a smooth function $\phi \in C_c^\infty(\mathbb{R})$ whose support is contained in a small enough neighborhood of 0 is a smooth function with support in the interior of the interval $[-L/2, L/2]$. Fix such a ϕ positive with integral equal to 1. Let $\phi_n(x) = n\phi(nx)$, and let $\eta_n = \phi_n * \xi_1$. One has

$$\widehat{\eta}_n(s) = \widehat{\phi}(s/n)\widehat{\xi}_1(s).$$

The functions $\widehat{\phi}(s/n)$ are bounded $|\widehat{\phi}(s/n)| \leq 1$ and converge pointwise to 1, thus the Lebesgue dominated convergence theorem shows that for n large enough, one has

$$\int |\widehat{\xi}_1(s) - \widehat{\eta}_n(s)|^2 \big(1 + \log(1 + s^2)\big)\, ds < \varepsilon/4. \tag{2.18}$$

Finally, since $\eta_n \in C_c^\infty((-L/2, L/2))$ it can be viewed as a smooth function on the circle obtained by identifying the end points of the interval $[-L/2, L/2]$ so that there exists a sequence $(a_k)_{k\in\mathbb{Z}}$ of rapid decay such that $\eta_n = \sum a_k U^k$. Equation (2.13) still holds after the change of variables and one gets the equality

$$\|\widehat{U}^k\|_1^2 = 4(\log\lambda)^2 \int \left|\sin(s\log\lambda)(\pi k - s\log\lambda)^{-1}\right|^2 \big(1+\log(1+s^2)\big)\, ds.$$

One has

$$\sin^2(s)s^{-2} \leq 2(1+s^2)^{-1},$$

and for any $a \in \mathbb{R}$,

$$1 + (s-a)^2 \leq 2(1+a^2)(1+s^2),$$

so that

$$\log\big(1+(s-a)^2\big) \leq \log 2 + \log(1+s^2) + \log(1+a^2).$$

This shows that $\|\widehat{U}^k\|_1^2 = O(\log|k|)$ and hence, since $\eta_n = \sum a_k U^k$ where the sequence $(a_k)_{k\in\mathbb{Z}}$ is of rapid decay, one can find N such that $\eta = \sum_{-N}^{N} a_k U^k$ fulfills

$$\int |\widehat{\eta}(s) - \widehat{\eta}_n(s)|^2 \big(1+\log(1+s^2)\big)\, ds < \varepsilon/4. \tag{2.19}$$

Combining (2.17)–(2.19), one obtains the required approximation. ∎

Proposition 2.3. *Let $\lambda > 1$. The quadratic form*

$$QW_\lambda : L^2\big([\lambda^{-1}, \lambda], d^*u\big) \to (-\infty, +\infty]$$

of (2.11) *fulfills*

$$QW_\lambda(f) = \liminf_{g_n \to f} QW_\lambda(g_n), \quad g_n \in \mathbb{C}[U, U^{-1}] \tag{2.20}$$

for any $f \in L^2([\lambda^{-1}, \lambda], d^*u)$.

Proof. By applying the lower semi-continuity of QW_λ one sees that in (2.20) the left-hand side is smaller than the right-hand side. The density of $\mathbb{C}[U, U^{-1}]$ in the domain of QW_λ for the graph-norm shown in Lemma 2.2, proves that if f is in the domain of QW_λ there exists a sequence g_n of elements of $\mathbb{C}[U, U^{-1}]$ converging to f in norm, and such that $QW_\lambda(f) = \lim_{g_n \to f} QW_\lambda(g_n)$. ∎

Corollary 2.4. *The lower bound of QW_λ is the limit, when $N \to \infty$, of the smallest eigenvalue of the restriction of QW_λ to the linear span E_N of the functions U^k for $|k| \leq N$.*

2.1.3. Basis of real functions in $\mathbb{C}[U, U^{-1}]$. In order to compute explicitly the smallest eigenvalue of the restriction of QW_λ to the linear span E_N of the functions U^k for $|k| \leq N$, as in Corollary 2.4, we first find a convenient orthonormal basis formed of real valued functions. We first consider the Hilbert space $L^2([-L/2, L/2]) \subset L^2(\mathbb{R})$ with the inner product defined by the formula

$$\langle \xi \mid \eta \rangle := \int_{-L/2}^{L/2} \overline{\xi(x)} \eta(x)\, dx.$$

An orthonormal real basis is, given by the constant function $\xi_0(x) = L^{-1/2}$ together with the functions $\xi_n(x)$, $n \in \mathbb{Z}$, $n \neq 0$, defined as follows

$$\begin{aligned} \xi_n(x) &:= (-1)^n \Big(\frac{2}{L}\Big)^{1/2} \cos\Big(\frac{2\pi n x}{L}\Big), \quad \forall n > 0 \\ \xi_n(x) &:= (-1)^n \Big(\frac{2}{L}\Big)^{1/2} \sin\Big(\frac{2\pi n x}{L}\Big), \quad \forall n < 0. \end{aligned} \tag{2.21}$$

We note the following simple facts:

Lemma 2.5. *Let $L > 0$, $\phi_j \in L^2([-L/2, L/2])$ and $\theta = \phi_1 * \phi_2^*$. Then*

(i) *The support of θ is contained in the interval $[-L, L]$, and for $t \in [0, L]$, one has*

$$\theta(t) = \int_{t-L/2}^{L/2} \phi_1(x) \overline{\phi_2(x-t)}\, dx, \quad \theta(-t) = \int_{t-L/2}^{L/2} \phi_1(x-t) \overline{\phi_2(x)}\, dx.$$

(ii) *If the functions ϕ_j are real, then*

$$\phi_1 * \phi_2^*(-t) = \phi_2 * \phi_1^*(t).$$

(iii) *If the functions ϕ_j are real, with ϕ_1 even and ϕ_2 odd, then for all $t \in \mathbb{R}$, one has*

$$\phi_1 * \phi_2^*(t) + \phi_2 * \phi_1^*(t) = 0.$$

Proof. (i) The function θ is given, using $\phi_2^*(x) = \overline{\phi_2(-x)}$, by

$$\theta(t) = \int_{\mathbb{R}} \phi_1(x) \overline{\phi_2(x-t)}\, dx, \quad t \in \mathbb{R}.$$

Since the integrand is not zero only if $x \in [-L/2, L/2]$ and $x - t \in [-L/2, L/2]$, one can restrict the integration in the interval $[t - L/2, L/2]$. The second equality follows using the equality $\theta^* = \phi_2 * \phi_1^*$.

(ii) Follows from $\theta^* = \phi_2 * \phi_1^*$.

(iii) Notice that $\phi_2^* = -\phi_2$ since ϕ_2 is real and odd, and $\phi_1^* = \phi_1$ since ϕ_1 is real and even, thus one derives

$$\phi_1 * \phi_2^* + \phi_2 * \phi_1^* = -\phi_1 * \phi_2 + \phi_2 * \phi_1 = 0. \qquad \blacksquare$$

It is convenient to rewrite the Weil sesquilinear form $QW(f,g) = \psi(f^* * g)$ using the natural invariance of the functional ψ under the symmetry $h^\sigma(u) := h(u^{-1})$. Thus,

$$\psi(h) = \psi^\#(h + h^\sigma), \quad h^\sigma(u) := h(u^{-1}), \tag{2.22}$$

where

$$\psi^\#(F) := W^\#_{0,2}(F) - W^\#_{\mathbb{R}}(F) - \sum W^\#_p(F) \tag{2.23}$$

with

$$W^\#_{0,2}(F) = \int_1^\infty F(x)(x^{1/2} + x^{-1/2})\, d^*x, \tag{2.24}$$

$$W^\#_{\mathbb{R}}(F) = \frac{1}{2}(\log 4\pi + \gamma)F(1) + \int_1^\infty \frac{x^{1/2}F(x) - F(1)}{x - x^{-1}}\, d^*x, \tag{2.25}$$

$$W^\#_p(F) = (\log p) \sum_{m=1}^\infty p^{-m/2} F(p^m). \tag{2.26}$$

Lemma 2.6. *With $\eta_n(u) := \xi_n(\log u)$, the η_j, $|j| \leq n$ form an orthonormal basis of E_n.*

(i) *The matrix of the Weil sesquilinear form is given by the following formula*

$$\begin{aligned} QW_\lambda(\eta_n, \eta_m) &= \sigma(n,m) = \psi^\#(h), \\ h(u) &= (\xi_n * \xi_m^* + \xi_m * \xi_n^*)(\log u), \end{aligned} \tag{2.27}$$

where $\psi^\#(h)$ is defined in (2.23).

(ii) *For $n \geq 0$, $m < 0$, one has*

$$(\xi_n * \xi_m^* + \xi_m * \xi_n^*)(y) = 0, \quad \forall y \in \mathbb{R}.$$

(iii) *For $nm > 0$, or $n = 0$ and $m \geq 0$, one has*

$$\xi_n * \xi_m^* = \xi_m * \xi_n^*.$$

Furthermore, the convolution $\xi_n * \xi_m^*(y)$ is an even function of y whose explicit description, for $y \in [0, L]$, is given in Table 1 whose general term gives the function $1/2(\xi_n * \xi_m^* + \xi_m * \xi_n^*)(y)$.

Proof. (ii) Follows from Lemma 2.5.

(iii) The table reported in (iii) is obtained by direct computation.

	$n>0$	$n=0$	$n<0$
$m>0, n\neq m$	$\frac{n\sin\left(\frac{2\pi ny}{L}\right)-m\sin\left(\frac{2\pi my}{L}\right)}{\pi(m^2-n^2)}$	$-\frac{\sin\left(\frac{2\pi my}{L}\right)}{\sqrt{2}\pi m}$	0
$m=n>0$	$\frac{(L-y)\cos\left(\frac{2\pi ny}{L}\right)}{L}-\frac{\sin\left(\frac{2\pi ny}{L}\right)}{2\pi n}$	$\emptyset$	$\emptyset$
$m=0$	$-\frac{\sin\left(\frac{2\pi ny}{L}\right)}{\sqrt{2}\pi n}$	$\frac{L-y}{L}$	0
$m<0, n\neq m$	0	0	$\frac{m\sin\left(\frac{2\pi ny}{L}\right)-n\sin\left(\frac{2\pi my}{L}\right)}{\pi(m^2-n^2)}$
$m=n<0$	$\emptyset$	$\emptyset$	$\frac{\sin\left(\frac{2\pi ny}{L}\right)}{2\pi n}+\frac{(L-y)\cos\left(\frac{2\pi ny}{L}\right)}{L}$

TABLE 1

(i) The formulas reported in (iii) show that all functions involved are in the domain of applicability $\mathcal{W}$ of the explicit formulas (see Section 2.1.1). Moreover, the terms of the explicit formulas correspond to the terms which enter in the definition (2.11) of the quadratic form QW_λ in Proposition 2.1. ∎

Lemma 2.6 (ii) shows that σ is a symmetric matrix and that

$$\sigma(n,m)=0, \quad \forall n\geq 0,\ m<0.$$

Thus, σ splits in two blocks $\sigma=\sigma^+\oplus\sigma^-$ which we shall informally call the "even" and "odd" matrices. They correspond to the partition $\mathbb{Z}=\{n\geq 0\}\cup\{n<0\}$ and one has

$$QW_\lambda = QW_\lambda^+\oplus QW_\lambda^-, \quad \sigma=\sigma^+\oplus\sigma^-. \tag{2.28}$$

This decomposition shows that the positivity of the Weil quadratic form can be tested working separately the cases of even functions (using the matrix σ^+) and odd functions (using σ^-). In the chosen basis η_n, the even case corresponds to considering elements of the basis indexed by $n\geq 0$, while the odd case involves the η_n's indexed by $n<0$.

2.1.4. The matrix $w_{0,2}(n,m)$. Next, we shall describe the contribution of the first two terms in (2.8) to the matrix $\sigma(m,n)$. The following lemma shows that these terms contribute by a rank one matrix to both the odd and the even matrices $\sigma^\pm$.

Lemma 2.7. *Let $n,m>0$ be positive integers, $\theta=\xi_m*\xi_n^*$, $F(x)=\theta(\log x)$. The following equality holds:*

$$\widehat{F}(i/2)+\widehat{F}(-i/2)=\frac{8e^{-L/2}(e^{L/2}-1)^2L^3}{(L^2+16\pi^2m^2)(L^2+16\pi^2n^2)}. \tag{2.29}$$

If $n, m < 0$ are negative integers, then one has

$$\widehat{F}(i/2) + \widehat{F}(-i/2) = -\frac{256\pi^2 L e^{-L/2}(e^{L/2}-1)^2 mn}{(L^2+16\pi^2m^2)(L^2+16\pi^2n^2)}. \tag{2.30}$$

Proof. We give the proof of (2.30); one proves (2.29) in a similar manner. One has

$$\begin{aligned}\widehat{F}(i/2) + \widehat{F}(-i/2) &= \int_{\mathbb{R}_+^*} F(x)(x^{1/2}+x^{-1/2})\, d^*x \\ &= \int_{\mathbb{R}} \theta(t)(e^{t/2}+e^{-t/2})\, dt \\ &= \int_0^\infty (\theta(t)+\theta(-t))(e^{t/2}+e^{-t/2})\, dt \\ &= \int_0^L (\theta(t)+\theta(-t))(e^{t/2}+e^{-t/2})\, dt.\end{aligned}$$

For $m \neq n$, Lemma 2.6 (iii) with $t \in [0, L]$ implies

$$\theta(t)+\theta(-t) = \frac{2}{(m^2-n^2)\pi}\Big(m\sin\Big(\frac{2\pi nt}{L}\Big) - n\sin\Big(\frac{2\pi mt}{L}\Big)\Big).$$

Furthermore, one also has

$$\int_0^L \sin\Big(\frac{2\pi nt}{L}\Big)(e^{t/2}+e^{-t/2})\, dt = -\frac{8\pi e^{-L/2}(e^{L/2}-1)^2 Ln}{L^2+16\pi^2n^2},$$

which gives

$$\widehat{F}(i/2) + \widehat{F}(-i/2) = \frac{2}{(m^2-n^2)\pi}\left(-\frac{128\pi^3 e^{-L/2}(e^{L/2}-1)^2 Lmn(m^2-n^2)}{(L^2+16\pi^2m^2)(L^2+16\pi^2n^2)}\right)$$

and this proves (2.30). When $m = n$, Lemma 2.6 (iii) with $t \in [0, L]$ gives

$$\theta(t)+\theta(-t) = \frac{1}{n\pi}\sin\Big(\frac{2\pi nt}{L}\Big) + 2\Big(1-\frac{t}{L}\Big)\cos\Big(\frac{2\pi nt}{L}\Big).$$

Then, one has

$$\int_0^L \Big(1-\frac{t}{L}\Big)\cos\Big(\frac{2\pi nt}{L}\Big)(e^{t/2}+e^{-t/2})\, dt = \frac{4e^{-L/2}(e^{L/2}-1)^2 L(L^2-16\pi^2n^2)}{(L^2+16\pi^2n^2)^2},$$

which gives

$$\begin{aligned}\widehat{F}(i/2) + \widehat{F}(-i/2) = &-\frac{8e^{-L/2}(e^{L/2}-1)^2 L}{L^2+16\pi^2n^2} \\ &+ \frac{8e^{-L/2}(e^{L/2}-1)^2 L(L^2-16\pi^2n^2)}{(L^2+16\pi^2n^2)^2}.\end{aligned}$$

This argument shows (2.30) using the equality

$$-(L^2+16\pi^2n^2) + (L^2-16\pi^2n^2) = -32\pi^2n^2.$$

∎

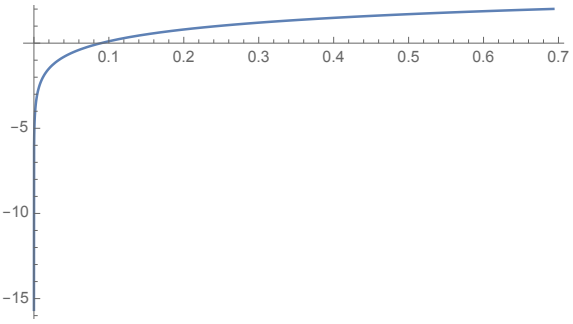

FIGURE 4
Coefficient of $\theta_{\mathrm{sym}}(0)/2$. Its value at $L = \log 2$ is 2.00963.

2.1.5. The sum $\sum W_p$. The contribution of the non-archimedean primes is given by (2.6), now written as

$$\sum W_p = \sum_{1<m\leq \exp(L)} \Lambda(m) m^{-1/2} (\xi_n * \xi_m^* + \xi_m * \xi_n^*)(\log m). \tag{2.31}$$

2.1.6. The functional $W_{\mathbb{R}}$. Let $\theta_{\mathrm{sym}}(t) = (\xi_n * \xi_m^* + \xi_m * \xi_n^*)(t)$, then (2.7) reads as

$$W_{\mathbb{R}} = \int_0^L \frac{\exp(x/2)\theta_{\mathrm{sym}}(x) - \theta_{\mathrm{sym}}(0)}{\exp(x) - \exp(-x)}\, dx - \theta_{\mathrm{sym}}(0) \int_L^\infty \frac{dx}{\exp(x) - \exp(-x)} + \frac{1}{2}(\gamma + \log(4\pi))\theta_{\mathrm{sym}}(0).$$

One has

$$\int_L^\infty \frac{dx}{\exp(x) - \exp(-x)} = \frac{1}{2} \log\Big(\frac{e^L + 1}{e^L - 1}\Big),$$

so that one obtains

$$W_{\mathbb{R}} = \frac{\theta_{\mathrm{sym}}(0)}{2}\Big(\gamma + \log\Big(4\pi \frac{e^L - 1}{e^L + 1}\Big)\Big) + \int_0^L \frac{\exp(x/2)\theta_{\mathrm{sym}}(x) - \theta_{\mathrm{sym}}(0)}{\exp(x) - \exp(-x)}\, dx. \tag{2.32}$$

Figure 4 shows that the coefficient of $\theta_{\mathrm{sym}}(0)/2$ is negative near the origin ($L = 0$), thus its contribution to the quadratic form QW is a positive one for small values of L, due to the minus sign in front of $W_{\mathbb{R}}^+$ (in (2.23)). This very same contribution becomes negative for larger values of L.

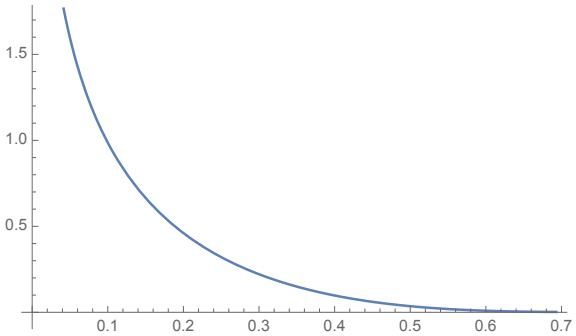

Figure 5
Positivity of the archimedean contribution to the even matrix for $L \in [0, \log 2]$. The smallest eigenvalue when $L = \log 2$ is ~ 0.00133.

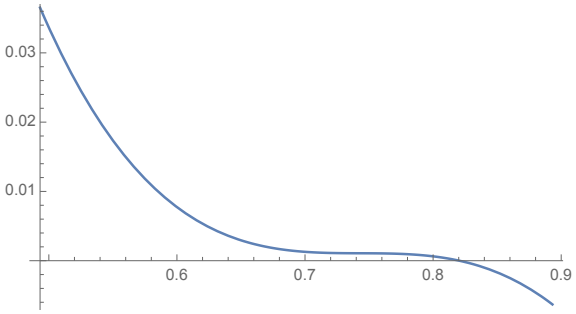

Figure 6
Change of sign of the smallest eigenvalue of the archimedean contribution to the even matrix for $L \in [\log 2 - 0.2, \log 2 + 0.2] \sim [0.493, 0.893]$.

2.2. Sensitivity of Weil positivity, archimedean place. The first fact we report from the numerical computations is that the archimedean contribution fails to remain positive when extended a bit beyond the value $L = \log 2$. In the two graphs above (Figures 5 and 6), we report the variation of the smallest eigenvalue for the even matrix σ^+, as the value of L approaches and then stretches a bit beyond $\log 2$. When one considers values of L in the interval $\log 2 \leq L < \log 3$, the contribution of the primes to the Weil quadratic form is only by $p = 2$, and of the form

$$W_p(F) = p^{-1/2} \log p \big(\theta(\log p) + \theta(-\log p)\big). \tag{2.33}$$

Figure 7 shows that adding the contribution of the prime 2 to the archimedean contribution restores the positivity of the even matrix σ^+. The graph is in terms of $\mu := \exp L$, and this choice of the variable is dictated by the fact that its integer prime power values play a crucial role in this study.

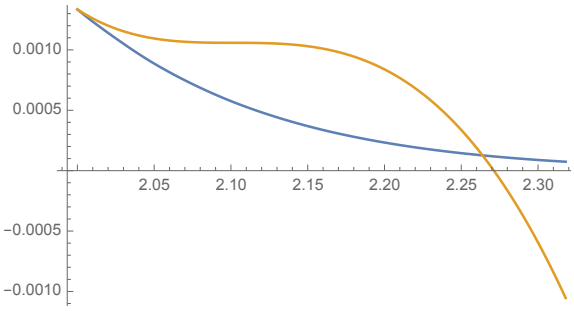

FIGURE 7
Change of sign of the smallest eigenvalue for the archimedean contribution alone, as a function of $\mu := \exp L$, near $\mu = 2$ (in yellow). After adding the contribution of the prime 2 the smallest eigenvalue of the even matrix is > 0 (in blue).

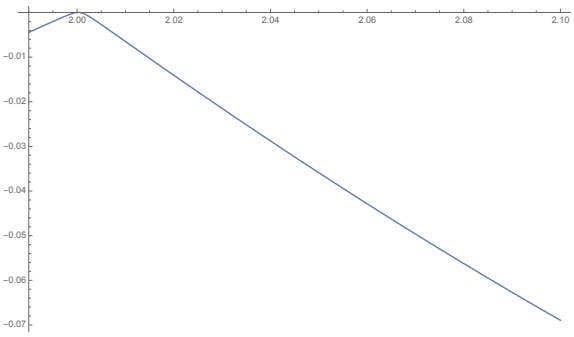

FIGURE 8
Sensitivity to the precise value $p = 2$.

2.3. Sensitivity of Weil positivity to the precise value $p = 2$. Figure 7 shows that beyond $\mu = 2$ the contribution (2.33) of the prime 2 first lowers the smallest eigenvalue in the interval $\exp L \in (2, 2.27)$ but then saves it from being negative. The value of the smallest eigenvalue of σ^+ for $\mu = 3$ is $< 6 \times 10^{-8}$. This suggests to use p as a variable in (2.33) and to test the sensitivity of Weil positivity to the precise value $p = 2$. To this end one fixes $L = \log 3$ (i.e. $\mu = 3$) and replaces 2 by a variable p in (2.33).

As Figure 8 shows, one finds that the smallest eigenvalue $\lambda(p)$ for $L = \log 3$ is negative for $p = 1.9999$ and also for $p = 2.0005$, so that the positivity requirement restricts the choice of p to an interval of size $< 10^{-3}$ around $p = 2$.

2.4. Change of sign of smallest eigenvalue. Beyond $p = 3$ the sign of the smallest eigenvalue of the sum of the contributions of ∞ and 2 to the even matrix σ^+ is reported in yellow in Figure 9. Once again we notice that its negative behavior beyond $\mu = 3$

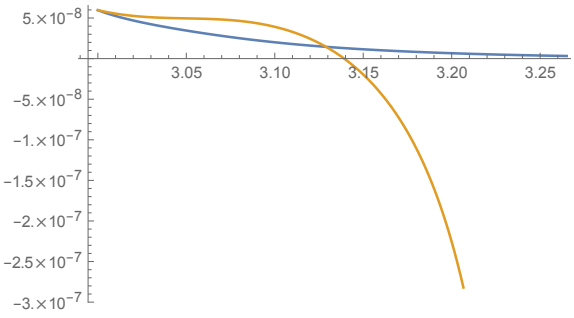

Figure 9
Change of sign of the smallest eigenvalue (in yellow) of the contributions of ∞ and 2 to the even matrix beyond $\mu = 3$. In blue, after adding the contribution of the prime 3: the total is > 0.

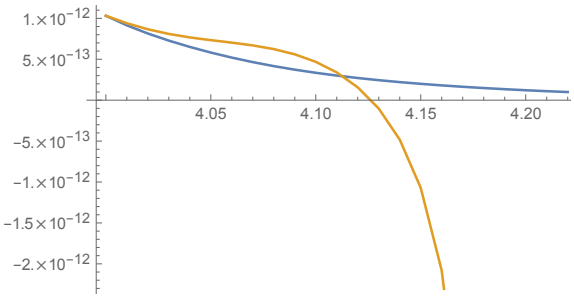

Figure 10
Change of sign of the smallest eigenvalue of the even matrix beyond 4: in yellow if one neglects the contribution of the prime power $4 = 2^2$, in blue if one does not. The smallest eigenvalue of the total contribution is > 0.

is "fixed" and the output (in blue in the figure) switches to be positive by adding the contribution of the prime 3.

When μ goes beyond the prime power $4 = 2^2$, the behavior of the smallest eigenvalue is similar to the earlier reported cases and is shown in Figure 10.

For $\mu \sim 5$ and $\mu \sim 7$, the behavior of the smallest eigenvalue for the even matrix σ^+ is similar to those shown in the earlier cases and is reported in Figures 11 and 12.

The following graphs (Figures 13–17) report the change of sign of the smallest eigenvalues for the odd matrices σ^-, and for the same choices of prime powers: namely near 2, 3, 4, 5 and 7.

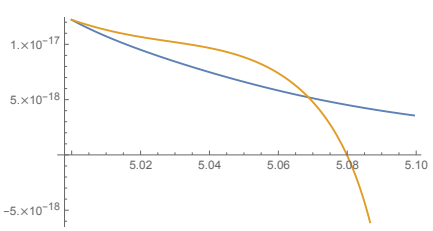

FIGURE 11
Going beyond $\mu = 5$ without (yellow) and with (blue) the contribution of the prime 5.

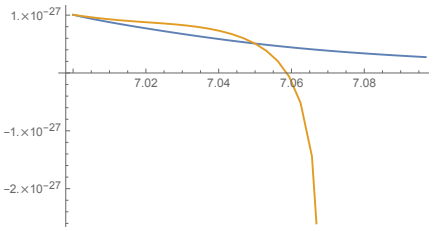

FIGURE 12
Going beyond $\mu = 7$ without (yellow) and with (blue) the contribution of the prime 7.

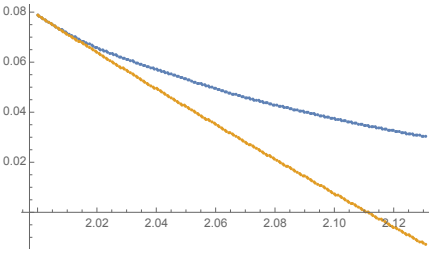

FIGURE 13
Odd case. Going beyond $\mu = 2$ without (yellow) and with (blue) the contribution of the prime 2.

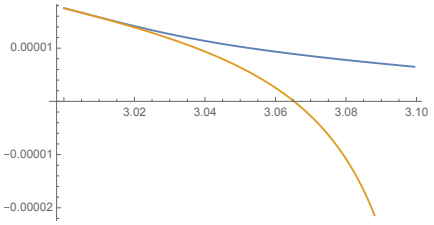

FIGURE 14
Odd case. Going beyond $\mu = 3$ without (yellow) and with (blue) the contribution of the prime 3.

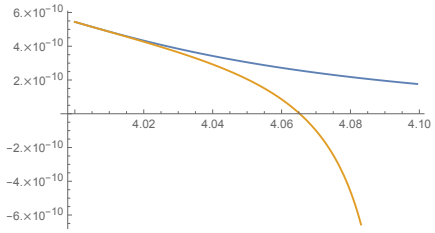

FIGURE 15
Odd case. Going beyond $\mu = 4$ without (yellow) and with (blue) the contribution of the prime power 4.

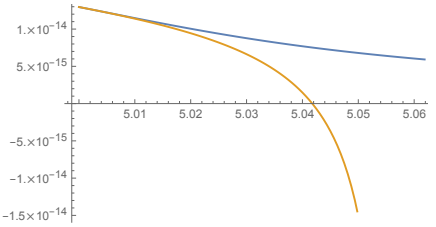

FIGURE 16
Odd case. Going beyond $\mu = 5$ without (yellow) and with (blue) the contribution of the prime 5.

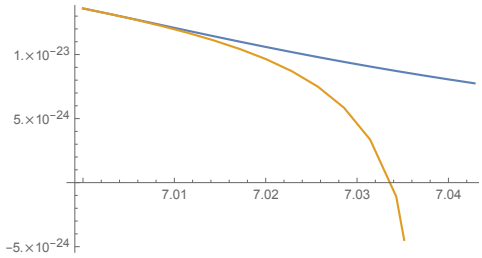

Figure 17
Odd case. Going beyond $\mu = 7$ without (yellow) and with (blue) the contribution of the prime 7.

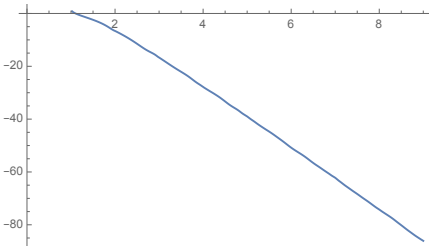

Figure 18
Decay of the log of the smallest eigenvalue of the even matrix as a function of $\mu = \exp L$.

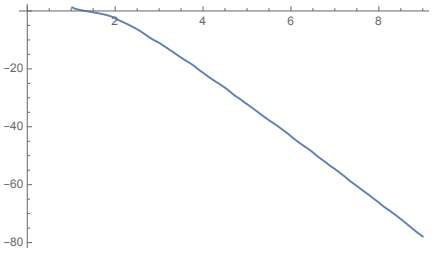

Figure 19
Decay of the log of the smallest eigenvalue of the odd matrix as a function of $\exp L$.

2.5. Semi-local Weil quadratic form, small eigenvalues. Pushing the computations further and increasing the precision, one obtains an estimate of the size of the smallest eigenvalue $s(L)$ of the even matrix, as a function of $\mu = \exp L$. One finds an exponential behavior, as reported in Figures 18 and 19, where $\log s(L)$ is plotted in terms of $\mu = \exp L$.

When one selects the small eigenvalues of the even matrix σ^+ and plots the graphs of the logarithm of their size, one finds (see Figure 20) that their number increases roughly like $\mu = \exp L$. For the odd matrix σ^-, the behavior is similar but with one less small eigenvalue, as shown in Figure 21.

Figures 22, 23 and 24 report the graphs of the eigenvectors of the quadratic form QW_λ^+ for the smallest, the second smallest, and the third smallest eigenvalues, respectively.

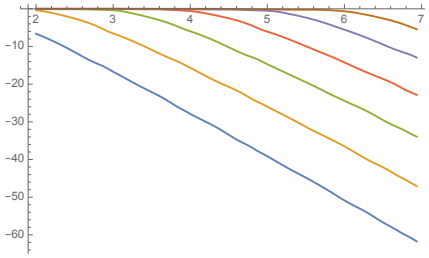

FIGURE 20
Decay of the log of the smallest eigenvalues of the even matrix σ^+ as a function of $\mu = \exp L$.

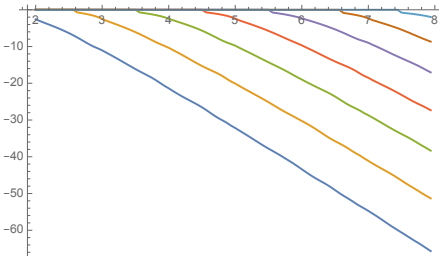

FIGURE 21
Decay of the log of the smallest eigenvalues of the odd matrix σ^- as a function of $\mu = \exp L$.

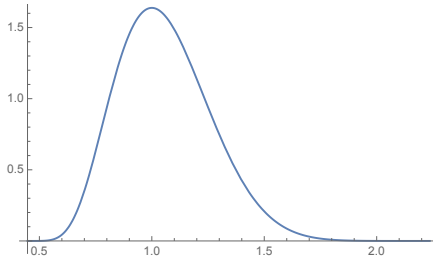

FIGURE 22
Eigenvector for the smallest eigenvalue of QW_λ^+ as function on $\mathbb{R}_+^*$.

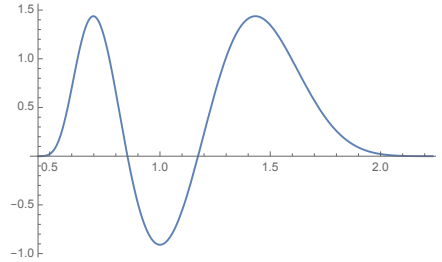

FIGURE 23
Eigenvector for the second smallest eigenvalue of QW_λ^+ as function on $\mathbb{R}_+^*$.

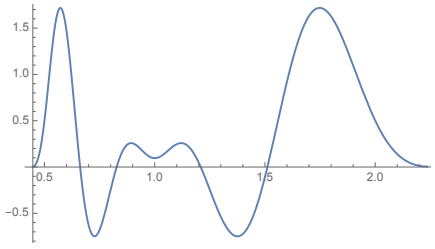

FIGURE 24
Eigenvector for the third smallest eigenvalue of QW_λ^+ as function on $\mathbb{R}_+^*$.

3. Eigenfunctions and the prolate projection $\Pi(\lambda, k)$

In this section we explain the existence of the very small eigenvalues of the Weil quadratic form QW_λ on test functions with support in an interval $[\lambda^{-1}, \lambda] \subset \mathbb{R}^*_+$. We start by recalling that if RH holds, then the Weil quadratic form restricted to functions with support in a finite interval has zero radical, since the number $N(r)$ of zeros of modulus at most r of the Fourier transform of a function f with compact support is of the order $N(r) = O(r)$ (see [8, Section 15.20 (2)]), while if f belonged to the radical of QW it would (assuming RH), vanish on all zeros of the Riemann zeta function whose number grows faster than $O(r)$. On the other hand, the radical of QW contains the range of the map $\mathcal{E}$ defined on the codimension two subspace $\mathcal{S}_0^{\mathrm{ev}} \subset \mathcal{S}(\mathbb{R})$ of even Schwartz functions fulfilling $f(0) = \widehat{f}(0) = 0$ by the formula ([4])

$$\mathcal{E}(f)(x) = x^{1/2} \sum_{n>0} f(nx). \tag{3.1}$$

It is thus natural to bring in (3.1) for the construction of functions g with support in $[\lambda^{-1}, \lambda] \subset \mathbb{R}^*_+$ which belong to the "near radical" of QW_λ, i.e. fulfill $QW_\lambda(g) \ll \|g\|^2$. The definition of $\mathcal{E}$ shows that if the support of the even function $f \in \mathcal{S}_0^{\mathrm{ev}}$ is contained in the interval $[-\lambda, \lambda] \subset \mathbb{R}$, then the support of $\mathcal{E}(f)$ is contained in $(0, \lambda] \subset \mathbb{R}^*_+$. On the other hand, by applying the Poisson formula (with $\widehat{f}$ the Fourier transform of f) one has

$$\mathcal{E}(\widehat{f})(x) = \mathcal{E}(f)(x^{-1}), \quad \forall f \in \mathcal{S}_0^{\mathrm{ev}}. \tag{3.2}$$

Thus, we see that λ^{-1} would be a lower bound of the support of $\mathcal{E}(f)$ if the support of the even function $\widehat{f} \in \mathcal{S}_0^{\mathrm{ev}}$ were contained in the interval $[-\lambda, \lambda] \subset \mathbb{R}$. However this latter inclusion is impossible since the Fourier transform of a function with compact support is analytic. In spite of this apparent obstacle in the construction, the work of Slepian and Pollack on band limited functions [13] provides a very useful approximate solution. The conceptual way to formulate their result is in terms of the pair of projections $\mathcal{P}_\lambda$ and $\widehat{\mathcal{P}}_\lambda$ in the Hilbert space $L^2(\mathbb{R})^{\mathrm{ev}}$ of square integrable even functions. The operator $\mathcal{P}_\lambda$ is the multiplication by the characteristic function of the interval $[-\lambda, \lambda] \subset \mathbb{R}$, and the projection $\widehat{\mathcal{P}}_\lambda$ is its conjugate by the (additive) Fourier transform $\mathbb{F}_{e_\mathbb{R}}$. These two projections have zero intersection but their "angle", – an operator with discrete spectrum – admits approximately $2\lambda^2$ very small eigenvalues whose associated eigenfunctions provide excellent candidates for the "approximate intersection" $\mathcal{P}_\lambda \cap' \widehat{\mathcal{P}}_\lambda$. In their work on signals transmission, Slepian and Pollack discovered that these eigenfunctions are exactly the prolate spheroidal wave functions which were already known to be solutions (by separation of variables) of the Helmoltz equation for prolate spheroids.

The basic result of Slepian and Pollack is the diagonalization of the positive operator $\mathcal{P}_\lambda \widehat{\mathcal{P}}_\lambda \mathcal{P}_\lambda$ in the Hilbert space $L^2([-\lambda, \lambda])$. They show that this operator commutes with the differential operator

$$(\mathbf{W}_\lambda \psi)(q) = -\partial\big((\lambda^2 - q^2)\partial\big)\psi(q) + (2\pi\lambda q)^2 \psi(q) \tag{3.3}$$

(here ∂ is the ordinary differentiation in one variable $q \in [-\lambda, \lambda]$ and the dense domain is that of smooth functions on $[-\lambda, \lambda]$). The operator $\mathbf{W}_\lambda$ (obtained by closing its domain in the graph norm) is self-adjoint and positive and its eigenfunctions are the prolate spheroidal wave functions. When considering the Weil quadratic form QW_λ evaluated on test functions with support in $[\lambda^{-1}, \lambda]$ we shall compare the eigenvectors associated to the extremely small eigenvalues with the range of the map $\mathcal{E}$ applied to linear combinations of eigenfunctions ψ of $\mathbf{W}_\lambda$ which belong to the approximate intersection $\mathcal{P}_\lambda \cap' \widehat{\mathcal{P}}_\lambda$ and vanish at zero. For this process, we only take the eigenfunctions ψ which are even functions of the variable q, and distinguish two cases since the action of the Fourier transform fulfills $\mathbb{F}_{e_\mathbb{R}} \psi \simeq \pm\psi$ on eigenfunctions ψ of $\mathbf{W}_\lambda$. The corresponding sign $\pm$ determines precisely the choice of an eigenvector for the even or odd matrix. In standard notation one sets

$$\psi_{m,\lambda}(x) := \mathrm{PS}_{2m,0}\Big(2\pi\lambda^2, \frac{x}{\lambda}\Big),$$

where $\psi_{m,\lambda}$ is a function on the interval $[-\lambda, \lambda]$ that one extends by 0 outside that interval. Its Fourier transform $\mathbb{F}_{e_\mathbb{R}}(\psi_{m,\lambda})$ is equal to $\chi_m \psi_{m,\lambda}$ on $[-\lambda, \lambda]$, where the scalar χ_m is very close to $(-1)^m$ provided that m is less than $2\lambda^2$. More precisely, $\mathbb{F}_{e_\mathbb{R}}(\psi_{m,\lambda})$ is computed using the equality

$$\int_{-1}^{1} \mathrm{PS}_{2m,0}(\gamma, \eta) \exp(i\gamma\eta\omega)\, d\eta = (-1)^m 2 S^{(1)}_{2m,0}(\gamma, 1)\, \mathrm{PS}_{2m,0}(\gamma, \omega)$$

for $\gamma = 2\pi\lambda^2$, $\omega = y/\lambda$. After changing variables to $\xi = \lambda\,\eta$, the equality above becomes

$$\int_{-\lambda}^{\lambda} \psi_{m,\lambda}(\xi) \exp(i\,2\pi\xi y)\, d\xi = (-1)^m 2\lambda S^{(1)}_{2m,0}(2\pi\lambda^2, 1)\psi_{m,\lambda}(y).$$

Given $\mu = \lambda^2$, one only retains the values of m for which the characteristic value

$$\chi(\mu, m) = 2\lambda S^{(1)}_{2m,0}(2\pi\mu, 1)$$

is almost equal to 1. This determines a collection $\{0, \ldots, \nu(\mu)\}$ of length approximately equal to 2μ, such that $\chi(\mu, m) \sim 1$ for $m \leq \nu(\mu)$. The formula $\nu(\mu) = 2\mu - 1$ works well when μ is a small half integer.

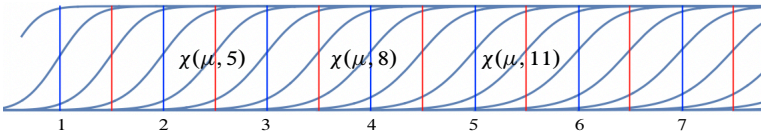

Figure 25
Graphs of the functions $\chi(\mu, m)$ as functions of μ.

In order to define the prolate projection we consider linear combinations of prolate functions which vanish at 0 and are given, for $n > 0$, by

$$\phi_{2n}(x) := \psi_{2n}(x)\psi_0(0) - \psi_0(x)\psi_{2n}(0),$$
$$\phi_{2n+1}(x) := \psi_{2n+1}(x)\psi_1(0) - \psi_1(x)\psi_{2n+1}(0).$$

For $1 < n \leq \nu(\mu)$, one may approximate $\mathbb{F}_{e_{\mathbb{R}}}(\phi_n)$ by $(-1)^n\phi_n$ and, using the Poisson formula, act as if $\mathcal{E}(\phi_n)$ would fulfill the equality

$$\mathcal{E}(\phi_n)(u^{-1}) = (-1)^n\mathcal{E}(\phi_n)(u).$$

We can then compute the components of $\mathcal{E}(\phi_n)$ in the orthogonal basis $\eta_j(u) = \xi_j(\log u)$ of $\mathcal{H} = L^2([\lambda^{-1}, \lambda], d^*x)$ (Lemma 2.6) which fulfill

$$\eta_j(u^{-1}) = -\eta_j(u) \quad \text{for } j < 0, \text{ and}$$
$$\eta_j(u^{-1}) = \eta_j(u) \quad \text{for } j \geq 0.$$

For $1 < n \leq \nu(\mu)$, the component of $\mathcal{E}(\phi_n)$ on η_j is non-zero only if η_j has the same parity as n, i.e. fulfills $\eta_j(u^{-1}) = (-1)^n\eta_j(u)$, and in this case is given by the formula

$$\mathcal{E}(\phi_n)_j \simeq 2\sum_{1\leq r<\lambda}\int_1^{\lambda/r} u^{1/2}\phi_n(ru)\eta_j(u)\,d^*u. \tag{3.4}$$

One computes all these components for $|j| \leq N$ with N large, and applies the Gram-Schmidt orthogonalization process (separately for the even and odd cases) to the obtained vectors in E_N. This process determines orthonormal vectors

$$\varepsilon_n \in E_N \subset \mathcal{H} = L^2\big([\lambda^{-1}, \lambda], d^*x\big) \quad \text{for } 1 < n \leq \nu(\mu)$$

which are, by construction, the natural candidate functions to be compared (up to sign) with the eigenfunctions of the semi-local Weil quadratic form QW_λ on E_N.

Definition 3.1. Let $k < \nu(\lambda^2)$. We define $\Pi(\lambda, k)$ as the orthogonal projection on the linear span of the vectors ε_n for $n \in \{2, \ldots, k+1\}$.

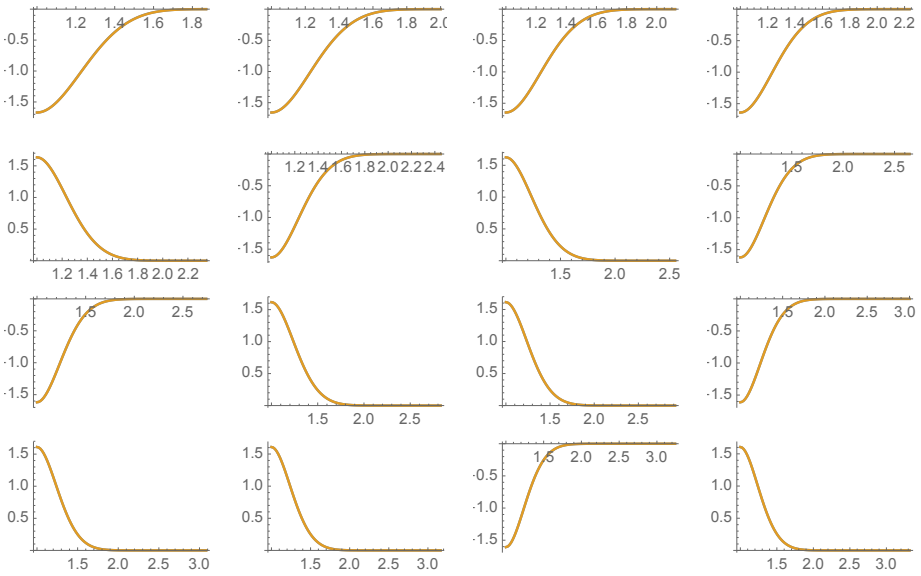

FIGURE 26
Agreement of eigenfunctions for the even matrix and the smallest eigenvalue, for the 16 values of μ between 3.5 and 11. For $\mu = 11$ the eigenvalue is 2.389×10^{-48}.

Let γ be the grading operator in $\mathcal{H} = L^2([\lambda^{-1}, \lambda], d^*x)$ which takes the values ± 1 on functions satisfying the equality $f(u^{-1}) = \pm f(u)$. By construction, the vectors ε_n are eigenvectors of γ and the following commutativity holds

$$\gamma\, \Pi(\lambda, k) = \Pi(\lambda, k)\, \gamma, \quad \forall \lambda, k. \tag{3.5}$$

The series of graphs reported here (Figures 26–37) display the coincidence of the ε_n with the actual eigenfunctions of the semi-local Weil quadratic form QW_λ for the smallest eigenvalues. When only one graph appears (in yellow the graph of the ε's) this means that the graphs of the two functions match with a high precision, otherwise the graph in blue of the eigenfunction is no longer hidden behind the yellow graph. Notice that the coincidence of ε_{2m} with the eigenfunction of the even matrix for its m-th eigenvalue is expected to hold only when this eigenvalue is small and hence only when $\mu > m$. Similarly, one expects the coincidence of ε_{2m+1} with the eigenfunction of the odd matrix for its m-th eigenvalue only when $\mu > m + 1$ (since the number of small eigenvalues of the odd matrix is one less than for the even one). We have nevertheless plotted the graphs for all half integer values of μ between 3.5 and 11 to show the mismatch of the graphs when μ is too small.

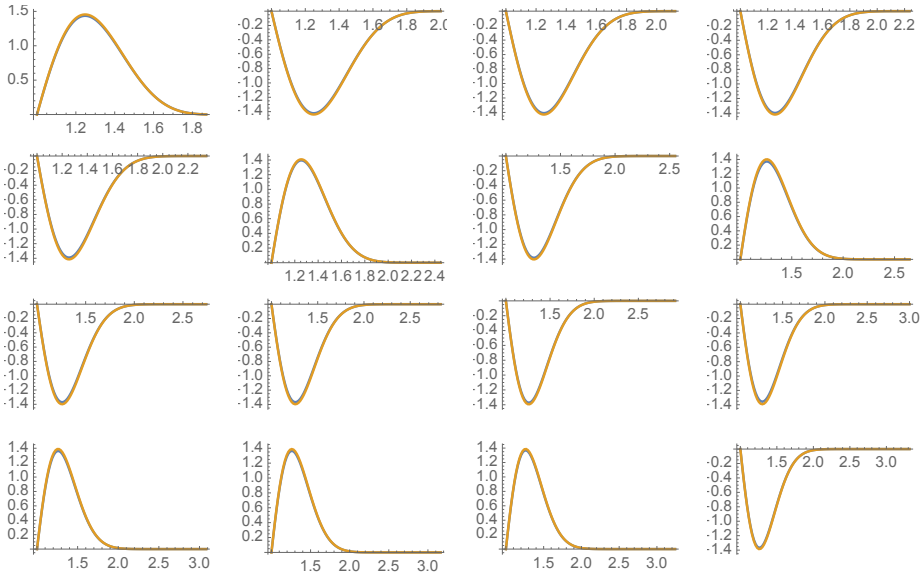

Figure 27
Agreement of eigenfunctions for the odd matrix and the smallest eigenvalue for the 16 values of μ between 3.5 and 11.

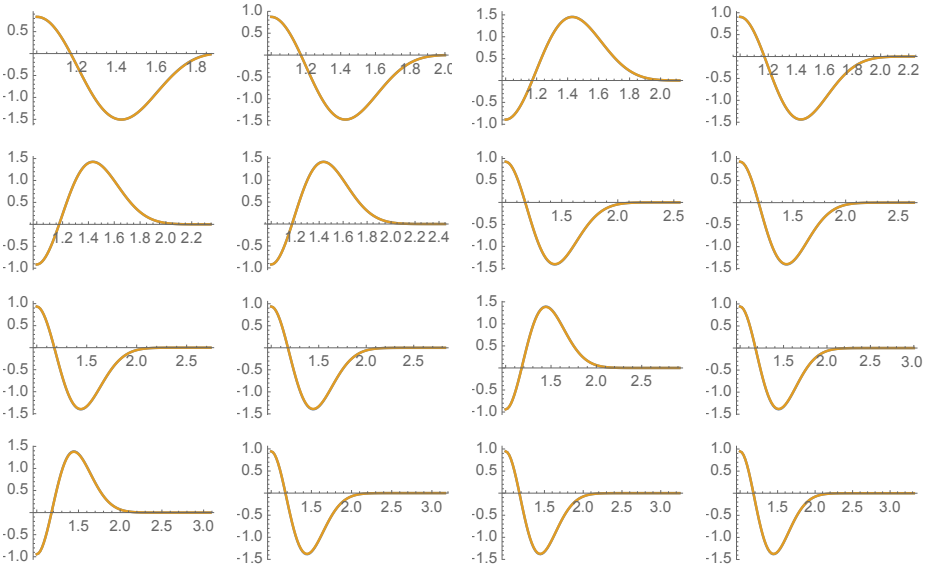

Figure 28
Agreement of eigenfunctions for the even matrix and the second smallest eigenvalue for the 16 values of μ between 3.5 and 11.

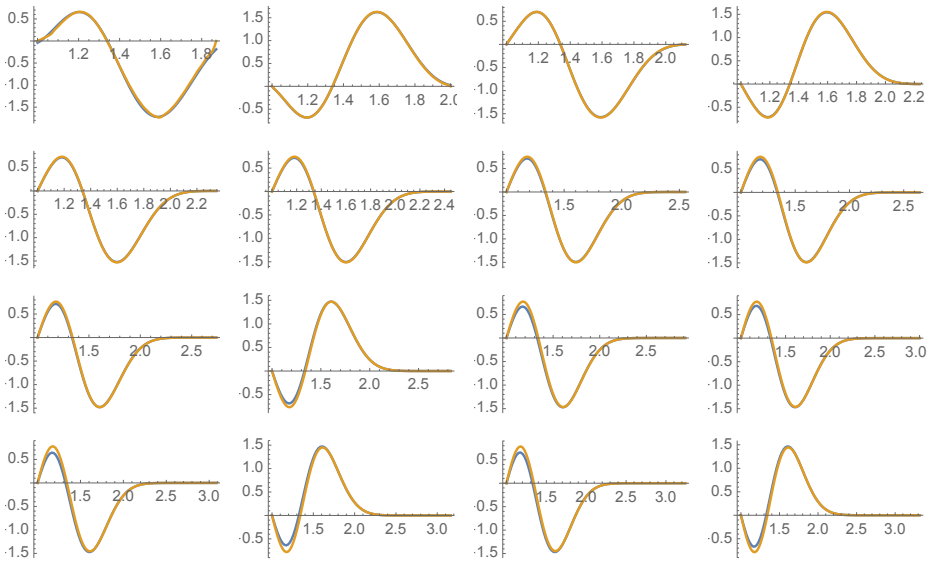

FIGURE 29
Agreement of eigenfunctions for the odd matrix and the second smallest eigenvalue for the 16 values of μ between 3.5 and 11.

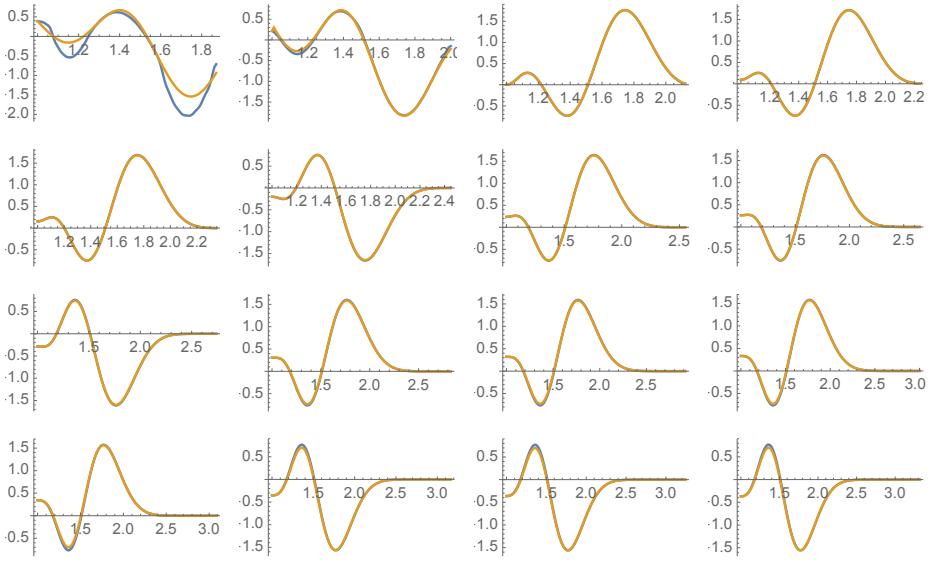

FIGURE 30
Agreement of eigenfunctions for the even matrix and the third smallest eigenvalue for the 16 values of μ between 3.5 and 11. They begin to agree around $\mu = 4$.

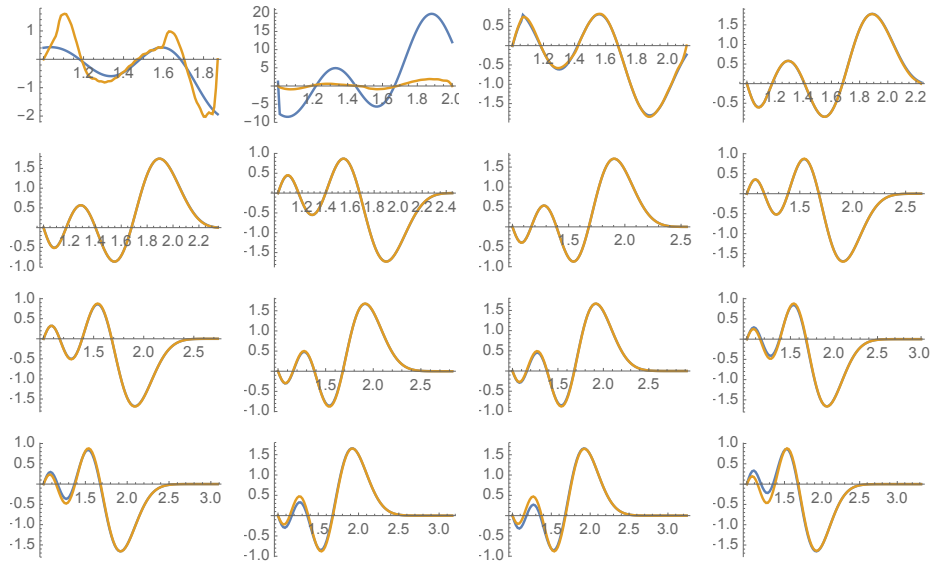

Figure 31
Agreement of eigenfunctions for the odd matrix and the third smallest eigenvalue for the 16 values of μ between 3.5 and 11. They begin to agree around $\mu = 4.5$.

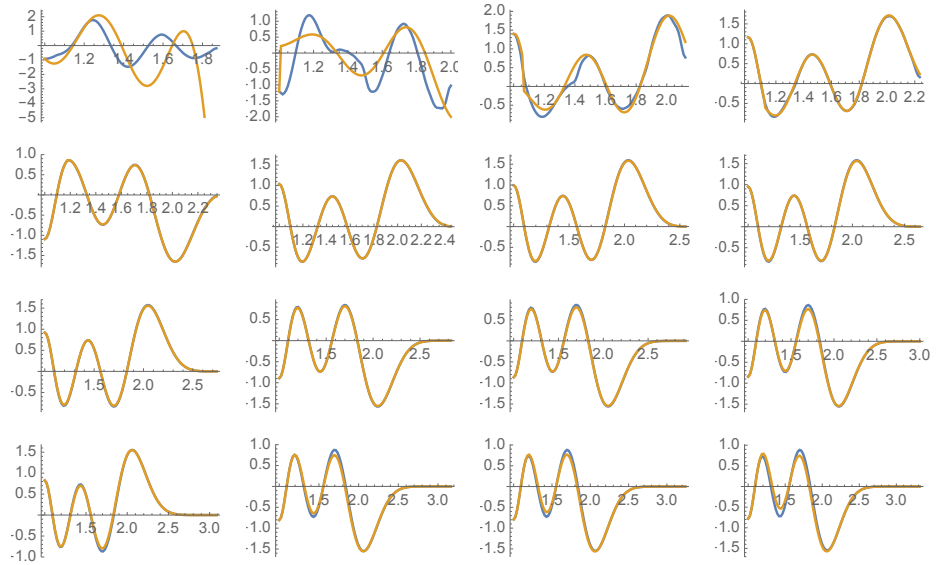

Figure 32
Agreement of eigenfunctions for the even matrix and the 4-th smallest eigenvalue for the 16 values of μ between 3.5 and 11. They begin to agree around $\mu = 5$.

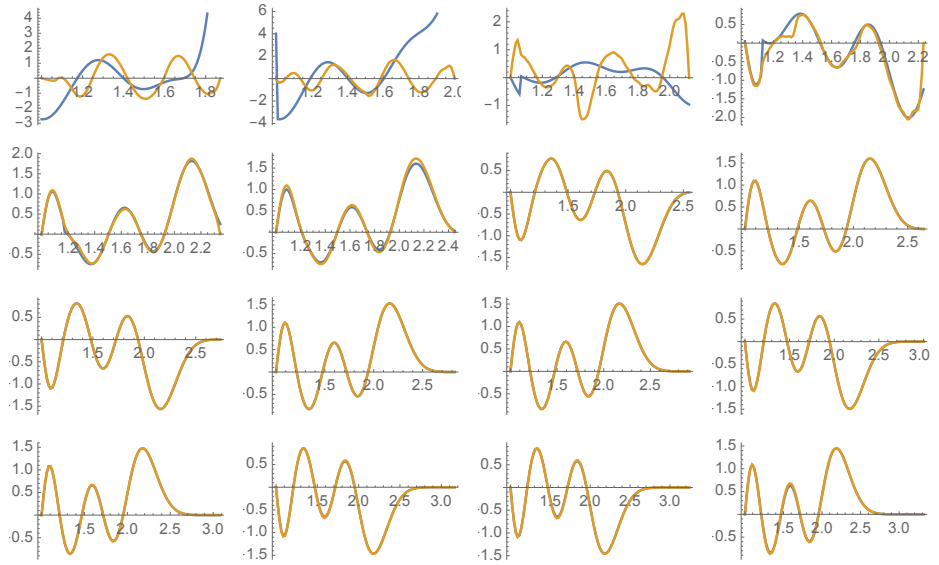

FIGURE 33
Agreement of eigenfunctions for the odd matrix and the 4-th smallest eigenvalue for the 16 values of μ between 3.5 and 11. They begin to agree around $\mu = 5.5$.

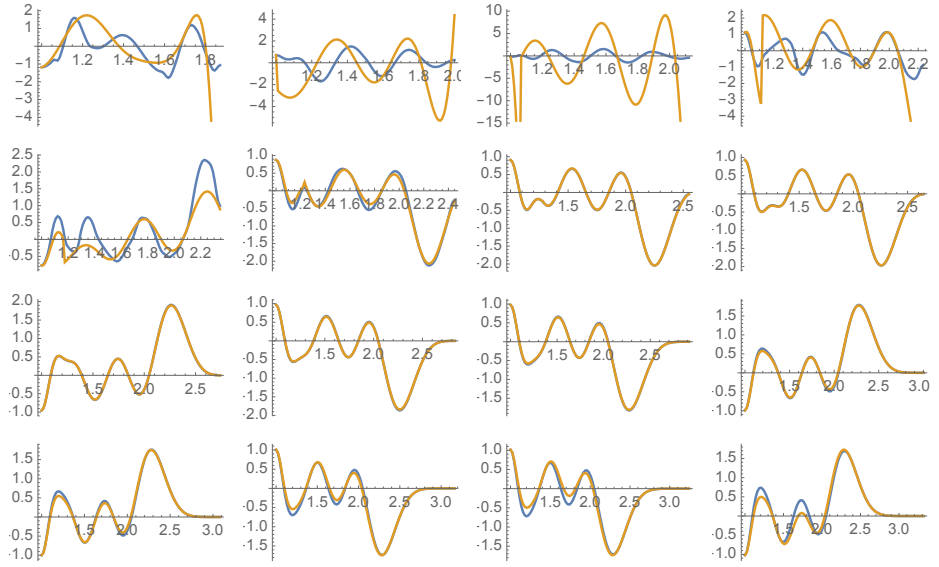

FIGURE 34
Agreement of eigenfunctions for the even matrix and the 5-th smallest eigenvalue for the 16 values of μ between 3.5 and 11. They begin to agree around $\mu = 6$.

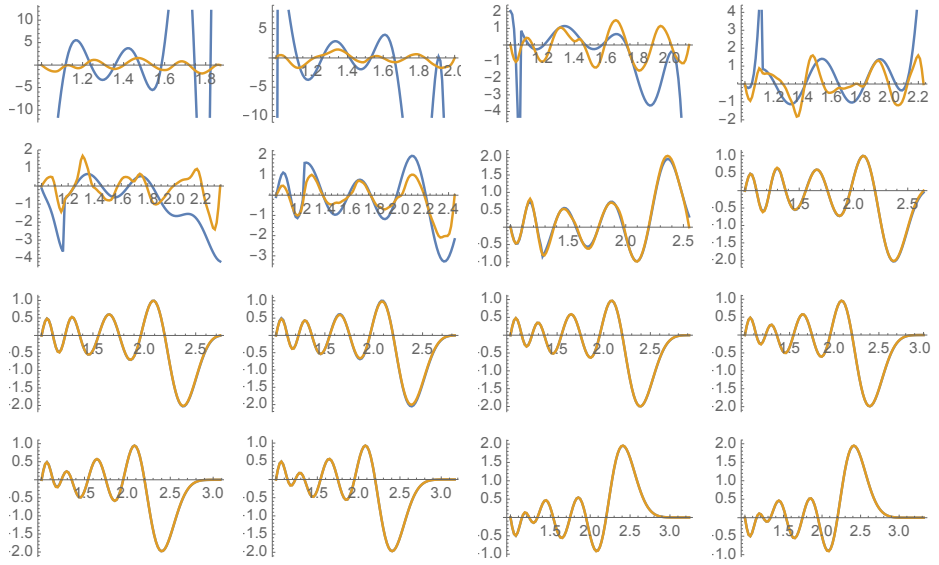

Figure 35
Agreement of eigenfunctions for the odd matrix and the 5-th smallest eigenvalue for the 16 values of μ between 3.5 and 11. They begin to agree around $\mu = 6.5$.

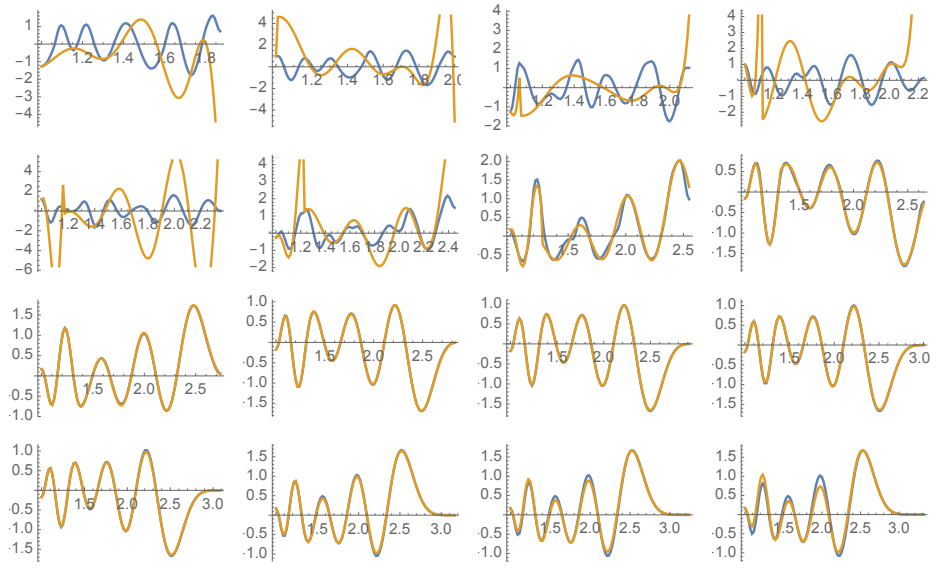

Figure 36
Agreement of eigenfunctions for the even matrix and the 6-th smallest eigenvalue for the 16 values of μ between 3.5 and 11. They begin to agree around $\mu = 7$.

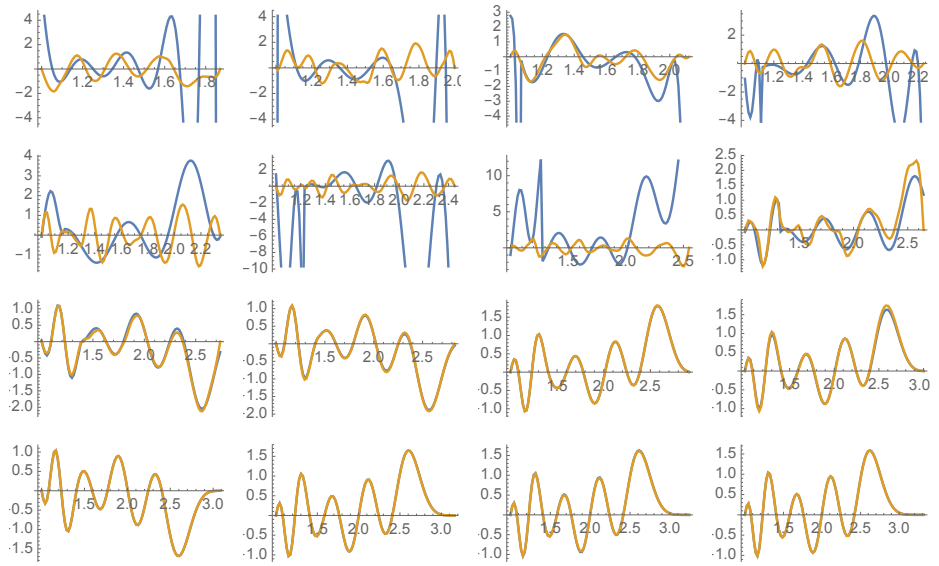

FIGURE 37
Agreement of eigenfunctions for the odd matrix and the 6-th smallest eigenvalue for the 16 values of μ between 3.5 and 11. They begin to agree around $\mu = 7.5$.

4. The spectral triple $\Theta(\lambda, k) = (\mathcal{A}(\lambda), \mathcal{H}(\lambda), D(\lambda, k))$

The spectral triple $\Theta(\lambda, k) = (\mathcal{A}(\lambda), \mathcal{H}(\lambda), D(\lambda, k))$ described in this section, whose spectrum has a remarkable similarity with the low lying zeros of the Riemann zeta function is defined through the action by multiplication of the algebra of smooth functions $\mathcal{A}(\lambda) := C^\infty(\mathbb{R}^*_+/\lambda^{2\mathbb{Z}})$ on the Hilbert space $\mathcal{H}(\lambda) := L^2(\mathbb{R}^*_+/\lambda^{2\mathbb{Z}}, d^*u)$. The operator $D(\lambda, k)$ is defined by the following formula

$$D(\lambda, k) := \big(1 - \Pi(\lambda, k)\big) \circ D_0(\lambda) \circ \big(1 - \Pi(\lambda, k)\big), \quad D_0(\lambda) := (-iu\partial_u). \tag{4.1}$$

This is a finite rank perturbation of the standard Dirac operator $D_0(\lambda)$, since by construction the range of the prolate projection $\Pi(\lambda, k)$ is contained in the domain of $D_0(\lambda)$, so that one derives

$$D(\lambda, k) = D_0(\lambda) - \Pi(\lambda, k)D_0(\lambda) - D_0(\lambda)\Pi(\lambda, k) + \Pi(\lambda, k)D_0(\lambda)\Pi(\lambda, k).$$

Proposition 4.1. *The operator $D(\lambda, k)$, combined with the action of periodic functions by multiplication in $L^2([-L/2, L/2])$ defines a spectral triple.*

Proof. The operator $D(\lambda, k)$ is a finite rank perturbation of $D_0(\lambda)$, thus by the Kato–Rellich theorem (see [9, Proposition 8.6]) it is essentially self-adjoint on any core

of $D_0(\lambda)$. The domain of $D(\lambda,k)$ is the same as the domain of $D_0(\lambda)$ and the boundedness of the commutator $[D(\lambda,k), f]$ follows from the boundedness of the perturbation. ∎

To compare the spectrum of $D(\lambda,k)$, for k just below the upper bound $\nu(\lambda^2) \sim 2\lambda^2$ (discussed in Section 3), with the zeros of the Riemann zeta function, one needs to select an appropriate range of eigenvalues for which the comparison is meaningful. By construction the number of eigenvalues of $D(\lambda,k)$ in the interval $[0, E]$ has the same asymptotic behavior as for $D_0(\lambda)$, and thus differs from the asymptotic behavior of the number $N(E)$ of zeros of the Riemann zeta function with imaginary part in the interval $[0, E]$, namely

$$N(E) = \#\{\rho \mid \zeta(\rho) = 0 \text{ and } 0 < \Im(\rho) \leq E\}. \tag{4.2}$$

This number is the sum of two contributions: $N(E) = \langle N(E)\rangle + N_{\mathrm{osc}}(E)$. The oscillatory term $N_{\mathrm{osc}}(E)$ is of order $\log E$ and, more importantly in this context, one knows that

$$\langle N(E)\rangle = \frac{E}{2\pi}\log\frac{E}{2\pi} - \frac{E}{2\pi}. \tag{4.3}$$

When considering the operator $D(\lambda,k)$, with k smaller and close to the upper bound $\nu(\lambda^2)$, we let $\mu = \lambda^2$ and we obtain the following proposition.

Proposition 4.2. *For $E = 2\pi\mu$, the number $N'(E)$ of non-zero eigenvalues of the operator $D(\lambda,k)$ in the interval $(0, E]$ fulfills $N'(E) \sim \langle N(E)\rangle$.*

Proof. It follows from (3.5) that $D(\lambda,k)\gamma = -\gamma D(\lambda,k)$, so that the number of eigenvalues of $D(\lambda,k)$ of absolute value less than E is $2N'(E)$ plus the dimension of the kernel of $D(\lambda,k)$. The spectrum of $D(\lambda,k)$ is a perturbation of the spectrum of $D_0(\lambda)$, i.e. of $\{2\pi k/L \mid k \in \mathbb{Z}\}$. The perturbation increases the dimension of the kernel of $D(\lambda,k)$ by the dimension of the projection $\Pi(\lambda,k)$, i.e. by $k \sim 2\mu$, up to a $\log\mu$ term. Thus, the number of non-zero eigenvalues of $D(\lambda,k)$ with absolute value less than E has an approximated size equal to

$$\begin{aligned} 2N'(E) &\sim \#\left(\left\{\frac{2\pi j}{L} \mid j \in \mathbb{Z}\right\} \cap [-E, E]\right) - 2\mu \\ &\sim 2\frac{EL}{2\pi} - 2\mu = 2\left(\frac{E}{2\pi}\log\frac{E}{2\pi} - \frac{E}{2\pi}\right) \end{aligned}$$

using $L = \log\mu$ and $\mu = \frac{E}{2\pi}$, which gives the expected estimate. ∎

4.1. Examples $\mu = 5.5, 6.5, 7.5, 8.5, 9.5, 10.5$. In this part we report some numerical evidence showing the close resemblance of the spectrum of $D(\lambda,k)$ with the low lying zeros of the Riemann zeta function, for a sample of small values of μ.

n	$\chi(5.5,n)$
5	0.99999999999647719857
6	0.99999999894391115741
7	0.99999980631702676769
8	0.99997809227622865324
9	0.99852183576050441685
10	0.95065832620623051607
11	0.57197061534624863399
12	0.13917453395457430353 9

TABLE 2

λ_j	ζ_j
14.781	14.1347
21.701	21.022
25.547	25.0109
29.345	30.4249
33.168	32.9351

TABLE 3

FIGURE 38
First 5 non-zero eigenvalues for the Dirac in upper line and imaginary parts of zeros of zeta in lower line.

4.1.1. $\mu = 5.5$. For $\mu = 5.5$, the cosine eigenvalues $\chi(5.5,n)$ are extremely close to 1 when $n = 0,1,2,3,4$ and given for the next values of n in Table 2. Thus, one derives that $\nu(5.5) = 10$, since the next eigenvalue 0.5719706153 is far from 1. One has $2\pi 5.5 \sim 34.5575$. Table 3 compares the positive eigenvalues $\lambda_j = \lambda_j(D(\lambda,k))$ of $D(\lambda,k)$ (reported on the left column) with the imaginary part ζ_j of the first zeros of the Riemann zeta function (right column). The spectral visualization is shown in Figure 38, with the zeta zeros at the bottom.

4.1.2. $\mu = 6.5$. For $\mu = 6.5$ the cosine eigenvalues $\chi(6.5,n)$ are extremely close to 1 when $n = 0,1,2,3,4,5,6$; for $7 \le n \le 14$, the values are reported in Table 4. Thus, one has $\nu(6.5) = 12$, since the next eigenvalue 0.5753409908 is far from 1. One has $2\pi 6.5 \sim 40.8407$. Once again, Table 5 reports the eigenvalues $\lambda_j = \lambda_j(D(\lambda,k))$ compared with the imaginary part ζ_j of the first zeros of the zeta function. The spectral visualization is shown in Figure 39 with the zero of the zeta function in the second line.

4.1.3. $\mu = 7.5$. The cosine eigenvalues $\chi(7.5,n)$ are extremely close to 1 for $n = 0,1,2,3,4,5,6,7,8$, and then given by Table 6. Thus, one has $\nu(7.5) = 14$ since the next eigenvalue 0.5780962979 is far from 1. One has $2\pi 7.5 \sim 47.1239$. Table 7 compares the eigenvalues $\lambda_j = \lambda_j(D(\lambda,k))$ with the imaginary part ζ_j of the first zeros of the zeta function. The spectral visualization is shown in Figure 40, with zeta zeros in the second line.

n	$\chi(6.5,n)$
7	0.99999999998668315975
8	0.99999999731589077585
9	0.99999963978717981581
10	0.99996808936687677767
11	0.99821407841789989100
12	0.94788066237037484836
13	0.57534099083086049406
14	0.14710511279564130503

Table 4

λ_j	ζ_j
13.936	14.1347
20.580	21.022
24.690	25.0109
30.194	30.4249
33.454	32.9351
36.826	37.5862
40.259	40.9187

Table 5

Figure 39
First 7 non-zero eigenvalues for the Dirac in upper line and imaginary parts of zeros of zeta in lower line.

n	$\chi(7.5,n)$
9	0.99999999996397226733
10	0.99999999453062631606
11	0.99999941709770526957
12	0.99995709581648305854
13	0.99792322303841470726
14	0.94552083061302325507
15	0.57809629788957190907
16	0.15383636015962926720

Table 6

λ_j	ζ_j	λ_j	ζ_j
15.060	14.1347	37.406	37.5862
21.683	21.022	40.514	40.9187
24.948	25.0109	43.643	43.3271
30.979	30.4249	46.658	48.0052
33.243	32.9351		

Table 7

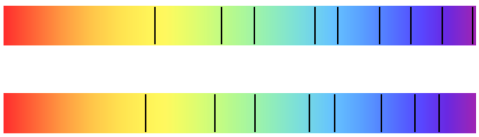

Figure 40
First 9 non-zero eigenvalues for the Dirac in upper line and imaginary parts of zeros of zeta in lower line.

n	$\chi(8.5,n)$
11	0.99999999992101000288
12	0.99999999034148375362
13	0.99999913999089362040
14	0.99994536408530411219
15	0.99764801726717553636
16	0.94347292951033144975
17	0.58041289343441020661
18	0.15967051202562674536

TABLE 8

λ_j	ζ_j	λ_j	ζ_j
14.887	14.1347	41.088	40.9187
20.778	21.022	43.741	43.3271
25.535	25.0109	46.685	48.0052
29.928	30.4249	49.910	49.7738
32.473	32.9351	52.845	52.9703
37.965	37.5862		

TABLE 9

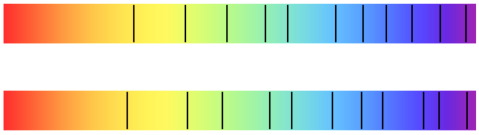

FIGURE 41
First 11 non-zero eigenvalues for the Dirac in upper line and imaginary parts of zeros of zeta in lower line.

4.1.4. $\mu = 8.5$. The $\chi(8.5,n)$ are extremely close to 1 for $n \leq 10$, and the next ones are given by Table 8. Thus, one has $\nu(8.5) = 16$, (the next eigenvalue 0.5804128934 is far from 1) and $2\pi 8.5 \sim 53.4071$. Table 9 reports the eigenvalues $\lambda_j = \lambda_j(D(\lambda,k))$ compared to the imaginary part ζ_j of the first zeros of the zeta function. The spectral visualization is reported in Figure 41, with the zeta zeros in the second line.

4.1.5. $\mu = 9.5$. For $\mu = 9.5$ the cosine eigenvalues $\chi(9.5,n)$ are extremely close to 1 when $0 \leq n \leq 12$, and for $13 \leq n \leq 20$ they are reported in Table 10. Thus, one has $\nu(9.5) = 18$, since the next eigenvalue 0.5824024487 is far from 1. One has $2\pi 9.5 \sim 59.6903$ and Table 11 reports the eigenvalues $\lambda_j = \lambda_j(D(\lambda,k))$ compared to the imaginary part ζ_j of the first zeros of the zeta function. The spectral visualization is shown in Figure 42, with the zeta zeros in the second line.

4.1.6. $\mu = 10.5$. For $\mu = 10.5$ the cosine eigenvalues $\chi(10.5,n)$ are extremely close to 1 when $0 \leq n \leq 14$, and for $15 \leq n \leq 22$ they are reported in Table 12. Thus, one has $\nu(10.5) = 20$, since the next eigenvalue 0.5841397980 is far from 1. One also has $2\pi 10.5 \sim 65.9734$. The table of eigenvalues (left column) compared to the first zeta zeros (right column) is Table 13. The spectral visualization is shown in Figure 43, with zeta zeros in the second line.

n	$\chi(9.5,n)$
13	0.99999999984990646525
14	0.99999998455736228573
15	0.99999881131048713492
16	0.99993308190344158164
17	0.99738707752987412262
18	0.94166650390462098514
19	0.58240244869697875785
20	0.16480962032526478957

Table 10

λ_j	ζ_j	λ_j	ζ_j
13.998	14.1347	43.050	43.3271
21.501	21.022	47.319	48.0052
25.121	25.0109	50.190	49.7738
30.689	30.4249	53.026	52.9703
33.583	32.9351	55.731	56.4462
37.813	37.5862	58.581	59.347
41.272	40.9187		

Table 11

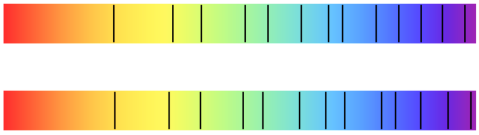

Figure 42
First 13 non-zero eigenvalues for the Dirac in upper line and imaginary parts of zeros of zeta in lower line.

n	$\chi(10.5,n)$
15	0.99999999974270022369
16	0.99999997703659571104
17	0.99999843436641476606
18	0.99992039045021729410
19	0.99713907784499135361
20	0.94005235637340584775
21	0.58413979804862029634
22	0.16935919615152177689

Table 12

λ_j	ζ_j	λ_j	ζ_j
14.450	14.1347	48.095	48.0052
21.455	21.022	50.346	49.7738
25.356	25.0109	53.272	52.9703
30.345	30.4249	56.050	56.4462
32.600	32.9351	58.737	59.347
37.410	37.5862	61.386	60.8318
40.387	40.9187	63.949	65.1125
42.895	43.3271		

Table 13

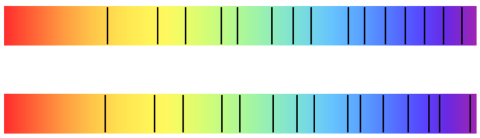

Figure 43
First 15 non-zero eigenvalues for the Dirac in upper line and imaginary parts of zeros of zeta in lower line.

4.2. Average discrepancy. For an objective comparison of the $N'(2\pi\mu)$ eigenvalues λ_j of size up to $2\pi\mu$, with the imaginary parts ζ_j of the zeros of the Riemann zeta function, one has at disposal the following three possible measures of the discrepancy:

(1) Mean absolute error.

$$A(\mu) := \frac{1}{N'(2\pi\mu)} \sum |\lambda_j - \zeta_j|.$$

When this error is computed for the values of μ used in the previous pages it gives the following list of values

$$A(5.5) = 0.635176, \quad A(6.5) = 0.44693, \quad A(7.5) = 0.528827,$$
$$A(8.5) = 0.456739, \quad A(9.5) = 0.395068.$$

(2) Root-mean-square deviation. It is defined as the square root of the average value of the square deviation

$$R(\mu) := \sqrt{\frac{1}{N'(2\pi\mu)} \sum (\lambda_j - \zeta_j)^2}.$$

This gives the following list of values

$$R(5.5) = 0.691088, \quad R(6.5) = 0.48858, \quad R(7.5) = 0.650648,$$
$$R(8.5) = 0.562489, \quad R(9.5) = 0.459776.$$

(3) Normalized root-mean-square deviation. This deviation is obtained by dividing the root-mean-square deviation by the diameter of the range of the variables. It is invariant under affine transformations and is thus a good measure of the discrepancy, usually expressed as a percentage. The diameter of the range of the variables is here equal to $2\pi\mu - 14$, and this gives the list,

$$NR(5.5) = 0.0375848, \quad NR(6.5) = 0.0185609, \quad NR(7.5) = 0.0205914,$$
$$NR(8.5) = 0.0148189, \quad NR(9.5) = 0.0103126, \quad NR(10.5) = 0.00995148.$$

These numbers show that the normalized root-mean-square deviation is steadily improving and reaches 1% (one percent) for $\mu = 9.5$ and then drops to less than one percent for $\mu = 10.5$.

5. Zeta zeros from eigenvalues of spectral triples

In the previous section we explored the low lying eigenvalues of the spectral triples $\Theta(\lambda, k) = (\mathcal{A}(\lambda), \mathcal{H}(\lambda), D(\lambda, k))$ for $k = 2\ell$ an even number as close as possible

to the boundary $\nu(\lambda^2) \sim 2\lambda^2$ of the allowed interval. These numerical results give evidence of a deep relation between the low lying spectrum $\lambda_n(D(\lambda,k))$ of these spectral triples and the low lying zeros of the Riemann zeta function. The dependence on the parameters (λ,k), and the difference between the growth of the eigenvalues and that of the zeros of zeta, show that the relation is certainly more subtle than a simple equality between the eigenvalues $\lambda_n(D(\lambda,k))$ and the imaginary part ζ_n of the zeros.

The main observation of this section is that, for any $n \in \mathbb{N}$ there are special values of the parameter λ at which the dependence of $\lambda_n(D(\lambda,k))$ on k disappears. For these special values of λ the common value of the $\lambda_n(D(\lambda,k))$ coincides with the imaginary part ζ_n of the n-th zero of the Riemann zeta function. Moreover, these special values of λ form a geometric progression whose scale factor is the exponential of π/ζ_n.

This observation was first experimentally tested and it will be fully and conceptually justified in Section 6.

We shall pursue 4 different criteria to detect these special values of λ. They are:

- Comparison of $\lambda_n(D(\lambda,2\ell))$ with $\lambda_n(D(\lambda,2\ell+1))$ (Section 5.1).
- Evolution of $\lambda_n(D(\lambda,k))$ as a function of λ (Section 5.2).
- Quantization criterion $x^{2iy}=1$ applied to the point $(\lambda,\lambda_n(D(\lambda,k)))$ (Section 5.3).
- How far is the eigenvector $\xi_n(D(\lambda,k))$ for $D(\lambda,k)$ from being an eigenvector of $D_0(\lambda)$?

The numerical tests of these criteria show their agreement, but the precision becomes very sharp when one applies the last criterion. Applying the last method for the small range of λ in the interval $(2,4)$ one obtains the agreement with the first 31 zeros ζ_n $(n \leq 31)$ of zeta with sufficient accuracy to assess the probability of a fortuitous coincidence at 10^{-50}.

5.1. The criterion $\lambda_n(D(\lambda,2\ell)) \sim \lambda_n(D(\lambda,2\ell+1))$. The first step in order to detect the special values of λ is to see what happens if one replaces $k=2\ell$ by the odd number $k+1=2\ell+1$. One sees that the positive eigenvalues $\lambda_n(D(\lambda,*))$ decrease and actually agree for special values of λ. We first briefly explain why

$$\lambda_n\big(D(\lambda,2\ell)\big) \geq \lambda_n\big(D(\lambda,2\ell+1)\big),$$

and then display some numerical results showing the coincidence for special values of λ. By construction, the kernel of $D(\lambda,k)$ contains the range of $\Pi(\lambda,k)$ and is thus at least of dimension k. Moreover, by (3.5) one has, for the grading γ of $\mathcal{H}(\lambda)$,

$$\gamma\, D(\lambda,k) = -D(\lambda,k)\,\gamma. \tag{5.1}$$

The kernel of the operator $D_0(\lambda)$ is one dimensional and given by the constant function 1_λ which is even (i.e. $\gamma(1_\lambda)=1_\lambda$). This implies that the graded index of the

operator $D_0(\lambda)$ is equal to 1. Then by stability of the index it follows that the graded index of the operator $D(\lambda, k)$ is also equal to 1. This means that the signature of the restriction of γ to the kernel of $D(\lambda, k)$ is 1 and hence that the dimension of $\ker(D(\lambda, k))$ is an odd number. Thus, for $k = 2\ell$ even, it is natural to expect this kernel to be of dimension $k + 1$. This entices one to compare the two non-zero eigenvalues $\lambda_n(D(\lambda, k))$ and $\lambda_n(D(\lambda, k + 1))$. By construction one has

$$\Pi(\lambda, k) < \Pi(\lambda, k + 1),$$

and we now explain why the positive eigenvalues of these operators, arranged in increasing order, fulfill the inequality

$$\lambda_n\big(D(\lambda, k + 1)\big) \leq \lambda_n\big(D(\lambda, k)\big), \quad \forall n, \lambda \tag{5.2}$$

Lemma 5.1. *Let A be a self-adjoint matrix of dimension N, and $E \subset \mathrm{Ker}\, A$ a subspace of its kernel. Then the positive eigenvalues $\mu_n(A)$ arranged in decreasing order fulfill*

$$\mu_n(A) = \max_{\substack{F \,|\dim F = n \\ F \perp E}} \min_{\substack{\xi \in F \\ \|\xi\| = 1}} \langle \xi \mid A\xi \rangle. \tag{5.3}$$

Proof. By the mini-max theorem of Courant–Fisher, one has

$$\mu_n(A) = \max_{F \,|\dim F = n} \min_{\substack{\xi \in F \\ \|\xi\| = 1}} \langle \xi \mid A\xi \rangle$$

and we need to show that the added condition that F is perpendicular to E does not change the maximum. It can only lower it and it is enough to check that the choice of F which reaches the maximum in the Courant–Fisher formula does fulfill $F \perp E$. Indeed this F is the linear span of the eigenvectors for eigenvalues $\mu_k(A)$ for $k \leq n$, and all these eigenvectors are orthogonal to the kernel of A since

$$\mu_k(A) \geq \mu_n(A) > 0$$

for $k \leq n$. ∎

Proposition 5.2. *Let $D \in M_N(\mathbb{C})$ be a self-adjoint matrix.*

(i) *Let $P \in M_N(\mathbb{C})$ be a projection (self-adjoint idempotent) and $Q = 1 - P$, $D_P := QDQ$. Then the positive eigenvalues of D_P arranged in decreasing order fulfill the equality*

$$\mu_n(D_P) = \max_{\substack{F \,|\dim F = n \\ F \perp P}} \min_{\substack{\xi \in F \\ \|\xi\| = 1}} \langle \xi \mid D\xi \rangle. \tag{5.4}$$

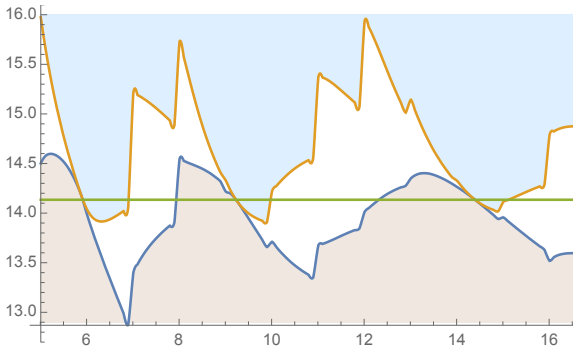

Figure 44
First eigenvalue, the lower graph is that of $\lambda_1(D(\lambda, k+1))$ and the upper graph is that of $\lambda_1(D(\lambda, k))$. The horizontal line is the imaginary part of the first zero of zeta.

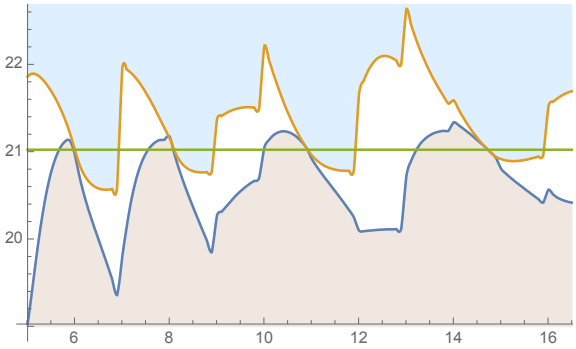

Figure 45
Second eigenvalue, the lower graph is that of $\lambda_2(D(\lambda, k+1))$ and the upper graph is that of $\lambda_2(D(\lambda, k))$. The horizontal line is the imaginary part of the second zero of zeta.

(ii) *Let $P_j \in M_N(\mathbb{C})$ be projections such that $P_1 \leq P_2$. Then with the notations of* (i), *the positive eigenvalues of D_{P_j} fulfill the inequality*

$$\mu_n(D_{P_2}) \leq \mu_n(D_{P_1}). \tag{5.5}$$

Proof. (i) By (5.3) applied to $A = D_P$ and $E = P(\mathbb{C}^N)$, one has

$$\mu_n(D_P) = \max_{\substack{F \,|\dim F = n,\\ F \perp E}} \min_{\substack{\xi \in F\\ \|\xi\|=1}} \langle \xi \mid D_P \xi \rangle,$$

and for $\xi \perp E$, one has $Q\xi = \xi$ so that

$$\langle \xi \mid D_P \xi \rangle = \langle \xi \mid QDQ\xi \rangle = \langle Q\xi \mid DQ\xi \rangle = \langle \xi \mid D\xi \rangle,$$

which gives (5.4).

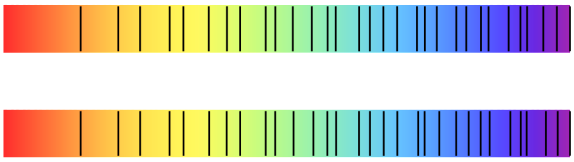

FIGURE 46
Using the criterion $\lambda_n(D(\lambda,k)) \sim \lambda_n(D(\lambda,k+1))$.

(ii) We apply (5.4) to $\mu_n(D_{P_j})$. The condition $F \perp P_2$ is more restrictive than $F \perp P_1$ so one obtains (5.5). ∎

Applying the criterion $\lambda_n(D(\lambda,k)) \sim \lambda_n(D(\lambda,k+1))$ to determine the relevant values of $\mu \in I = [5, 16.5]$, i.e. by minimizing the difference $\lambda_n(D(\lambda,k)) - \lambda_n(D(\lambda,k+1))$ on the finite set of $\mu \in \frac{1}{10}\mathbb{Z} \cap I$, one obtains the approximate list of the first 31 zeros of zeta shown in Figure 46.

5.2. Continuous evolution of non-zero eigenvalues for a fixed number of prolate conditions. When dealing with the operators $D(\lambda,k)$, with k close to the largest allowed value $\nu(\lambda^2) \sim 2\lambda^2$ one introduces necessarily a discontinuity due to the discrete nature of the variable k. To avoid it one can, for fixed k, consider the dependence of the eigenvalues $\lambda_n(D(\lambda,k))$ as long as λ is sufficiently large so that $k < \nu(\lambda^2)$. One finds that for the values $\ell = 2, 3$, the $\lambda_n(D(\lambda,2\ell))$ agree around $\mu \sim 3.8$ and that their common value is close to ζ_1. This fact is all the more remarkable that when $\mu < 4$, i.e. $\lambda < 2$ there is no summation involved in the (3.4). For $\ell = 3, 4, 5$, the $\lambda_n(D(\lambda,2\ell))$ agree around $\mu \sim 5.95$ and again we find that their common value is close to ζ_1. For $\ell = 5, 6, 7, 8$, the $\lambda_n(D(\lambda,2\ell))$ agree around $\mu \sim 9.2$ and again their value is close to ζ_1. For $\ell = 8, 9, 10, 11, 12, 13$ the $\lambda_n(D(\lambda,2\ell))$ agree around $\mu \sim 14.4$ and their value is close to ζ_1. The special values of μ at which the graphs meet appear to form a geometric progression. One finds that the ratio of consecutive terms is $\sim \exp(2\pi/\zeta_1)$ and, more generally that for the n-th eigenvalue the special values of μ form a geometric progression with scale ratio $\sim \exp(2\pi/\zeta_n)$ where ζ_n is the imaginary part of the n-th zero of zeta. These "experimental" facts will be theoretically explained by Theorem 6.4.

5.3. Quantization of length $\log \mu$. The fact that many graphs of the eigenvalues $\lambda_n(D(\lambda,k))$ meet at some specific points of the plane suggests that one could push the comparison even further and compare these points with the spectrum of the unperturbed operator $D_0(\lambda)$. In terms of the coordinates (x, y), where $x = \mu = \lambda^2$ and $y = \lambda_n(D(\lambda,k))$, the spectrum of $D_0(\lambda)$ is characterized by the quantization condition $x^{iy} = 1$. The subset of the plane defined by this condition is the union of the graphs of the functions $2\pi n/\log x$.

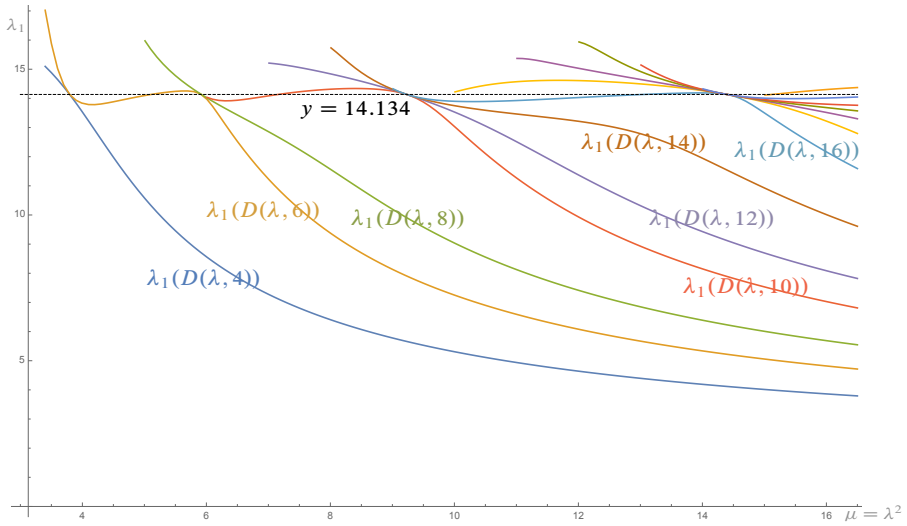

Figure 47
Evolution of the first non-zero eigenvalue of $D(\lambda, 2\ell)$. The dashed horizontal line is the value of the imaginary part ζ_1 of the first zero of zeta.

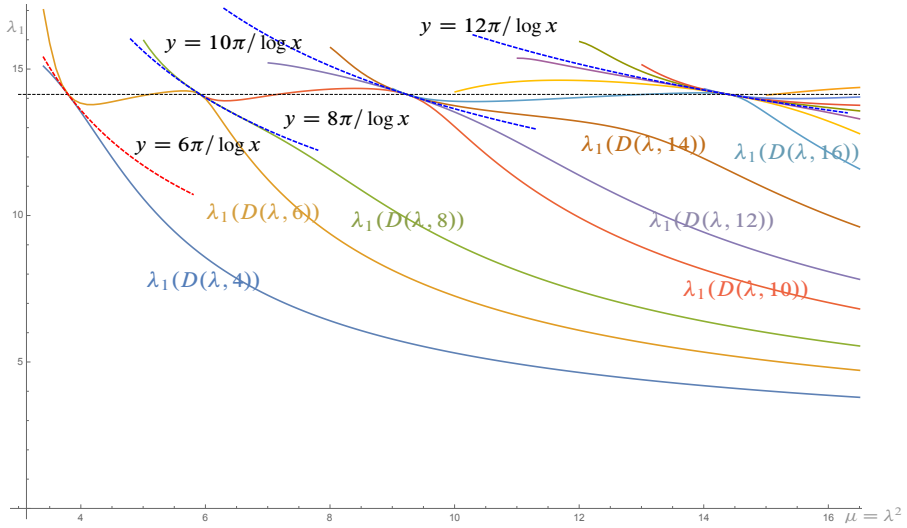

Figure 48
Coincidence with solutions of $x^{iy} = 1$.

Figure 48 shows a perfect agreement between these graphs and the meeting points of the eigenvalue graphs. Independently of this result, one can measure how far the

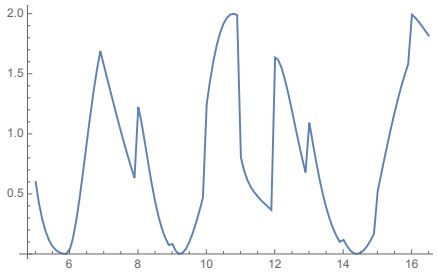

FIGURE 49
Graph of $|\mu^{i\lambda_1(\mu)} - 1|$.

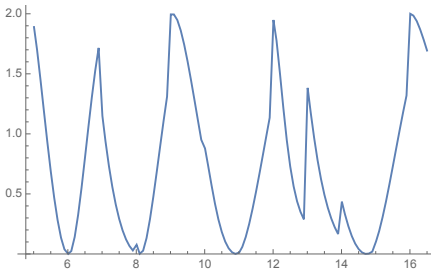

FIGURE 50
Graph of $|\mu^{i\lambda_2(\mu)} - 1|$.

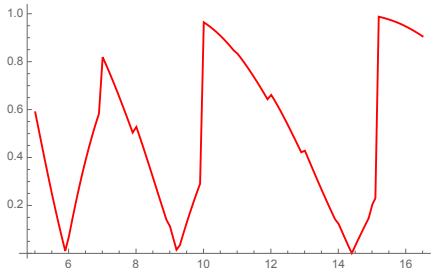

FIGURE 51
Distance of eigenvector of $D(\lambda, k)$ for λ_1 to eigenvectors of $D_0(\lambda)$.

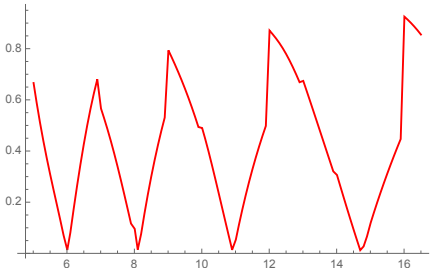

FIGURE 52
Distance of eigenvector $\xi_2(D(\lambda, k))$ to eigenvectors of $D_0(\lambda)$.

point $(\mu, \lambda_n(D(\lambda, k))$ is from fulfilling the quantization condition by writing it in the form

$$\mu^{i\lambda_n(D(\lambda,k))} = 1 \iff |\mu^{i\lambda_n(D(\lambda,k))} - 1| = 0,$$

and by plotting the graphs of these functions for each integer n. They are shown in Figure 49 for $n = 1$ and in Figure 50 for $n = 2$. The key fact here is that the values of μ at which these functions vanish coincide with the previously determined values where $\lambda_1(D(\lambda, k+1)) \sim \lambda_1(D(\lambda, k))$ of Figures 44 and 45.

5.4. The criterion of common eigenvector for $D(\lambda, k)$ and $D_0(\lambda)$. The agreement of the quantization with the meeting points of the graphs of the eigenvalues suggests that all the eigenvectors of the $D(\lambda, k)$ involved agree with each other and are in fact eigenvectors of the unperturbed operator $D_0(\lambda)$. This gives a very strong criterion obtained by measuring the Hilbert space distance of an eigenvector $\xi_n(D(\lambda, k))$ for $D(\lambda, k)$ with the eigenvector of $D_0(\lambda)$ which has the same rotation number. In Figures 51 and 52 the norm of the difference is plotted and one gets the agreement of the zeros with the values determined by the three previous criteria. Finally, Figure 53

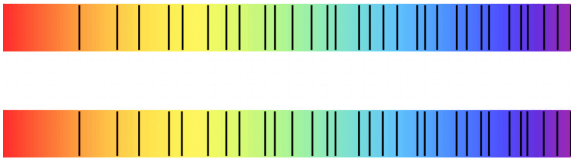

Figure 53
Using the criterion $\xi_n(D(\lambda,k))$ eigenvector of $D_0(\lambda)$, one obtains the 31 eigenvalues compared above with the imaginary parts of the first 31 zeros of the Riemann zeta function.

compares the first 31 eigenvalues selected using the last criterion with the imaginary parts of the first 31 zeros of the Riemann zeta function.

Remark 5.3. By construction the integers m involved in the construction of the operator $D(\lambda,k)$ (in the sum (3.4) involved in the projection $\Pi(\lambda,k)$) are limited to $m<\lambda$ while Proposition 4.2 specifies the range ($|E|\leq 2\pi\mu$, $\mu=\lambda^2$) where the eigenvalues of $D(\lambda,k)$ compare with the imaginary parts of zeros of the Riemann zeta function. It is remarkable that the above restriction on the involved integers coincides exactly with the restriction in the partial sums $\sum_{n\leq\lambda} n^{-s}$ occurring in the Riemann–Siegel formula for the approximate value of $\zeta(s)$, $s=\frac{1}{2}+iE$ (see [1] and [7, Section 6.1]).

6. ζ-cycles

The aim of this section is to provide a theoretical explanation for the numerical computations reported in the previous part of this paper, and in particular to give a theoretical justification for the close similarity of the spectrum of the operator $D(\lambda,k)$ in the spectral triple $\theta(\lambda,k)$ (see Section 4) and the low lying zeros of the Riemann zeta function. The goal we shall pursue here is to relate these intriguing numerical results with the spectral realization of the zeros of the Riemann zeta function, as developed in [4]. The new theoretical concept emerging is that of a ζ-cycle C. In the following part we first explain how to define scale invariant Riemann sums for functions defined on $[0,\infty)$ with vanishing integral. This technique is then implemented in the definition of a linear map $\Sigma_\mu\mathcal{E}\colon\mathcal{S}_0^{\mathrm{ev}}\to L^2(C)$ which plays a central role in this development and enters in the definition of the ζ-cycle (Definition 6.1). In Section 6.2 we prove that ζ-cycles are stable under finite covers, and finally we state and prove the main result of this paper, namely Theorem 6.4. This result naturally selects a family of Hilbert spaces $\mathcal{H}(L):=\Sigma_\mu\mathcal{E}(\mathcal{S}_0^{\mathrm{ev}})^\perp$ naturally associated to the critical zeros of the Riemann zeta function.

6.1. Scale invariant Riemann sums and the map $\Sigma_\mu \mathcal{E}$. Let $\mu > 1$ and Σ_μ be the linear map defined on functions $g: \mathbb{R}_+^* \to \mathbb{C}$ by the following formula

$$(\Sigma_\mu g)(u) := \sum_{k\in\mathbb{Z}} g(\mu^k u). \tag{6.1}$$

This definition makes sense pointwise provided g decays fast enough at 0 and ∞ in $\mathbb{R}_+^*$. The map $\mathcal{E}$ is defined as follows

$$(\mathcal{E} f)(u) := u^{1/2} \sum_{n>0} f(nu). \tag{6.2}$$

It is, by construction, proportional to a Riemann sum for the integral of f.

We let $\mathcal{S}_0^{\mathrm{ev}}$ be the linear space of real valued even Schwartz functions $f \in \mathcal{S}(\mathbb{R})$ such that

$$f(0) = 0 = \int f(x)\, dx.$$

The following lemma describes the "well-behavior" of the map $\mathcal{E}$.

Lemma 6.1. *Let f be a function of bounded variation on $(0,\infty)$, of rapid decay for $u \to \infty$, $O(u^2)$ when $u \to 0$, and such that*

$$\int_0^\infty f(t)\, dt = 0.$$

Then the following properties hold:

(i) *$\mathcal{E}(f)(u)$ is well-defined pointwise, is $O(u^{1/2})$ when $u \to 0$ and of rapid decay for $u \to \infty$.*

(ii) *The series (6.1) defining $\Sigma_\mu \mathcal{E}(f)$ is geometrically convergent, and defines a bounded measurable function on $\mathbb{R}_+^*/\mu^{\mathbb{Z}}$.*

Proof. (i) The sum

$$S(u) := u \sum_{n=0}^{\infty} f(nu)$$

is a Riemann sum for the integral

$$\int_0^\infty f(x)\, dx = 0.$$

One has $f(0) = 0$, and the following equality holds

$$u \sum_{n=0}^{\infty} f(nu) = -\sum_{n=0}^{\infty} \int_{nu}^{(n+1)u} \big((n+1)u - t\big)\, df(t)$$

since integration by parts in the Stieltjes integral shows that

$$\int_{nu}^{(n+1)u} \big((n+1)u - t\big)\, df(t) = \int_{nu}^{(n+1)u} f(t)\, dt - uf(nu),$$

while

$$\int_0^\infty f(t)\, dt = 0$$

by hypothesis. Since $|((n+1)u - t)| \leq u$ for $t \in [nu, (n+1)u]$, one obtains the upper-bound

$$\left| \sum_0^\infty f(nu) \right| \leq \sum_{n=0}^\infty \int_{nu}^{(n+1)u} |df(t)|.$$

The integral of the measure $|df(t)|$ is finite since f is of bounded variation. We thus derive

$$\left| \sum_{n=0}^\infty f(nu) \right| \leq \int_0^\infty |df(t)|$$

and from this it follows that $|\mathcal{E}(f)(u)| = O(u^{1/2})$ for $u \to 0$.

(ii) Since $f(u)$ is of rapid decay for $u \to \infty$, one has $|f(u)| \leq Cu^{-N}$, $N > 1$ and this implies

$$\sum_{n \geq 1} |f(nu)| \leq Cu^{-N} \sum_{n \geq 1} n^{-N} = C' u^{-N}.$$

Thus, $\mathcal{E}(f)(u)$ is of rapid decay for $u \to \infty$. Let $u \in [\lambda^{-1}, \lambda]$. The terms of the series

$$\sum_{\mathbb{Z}} \mathcal{E}(f)(\mu^k u)$$

converge geometrically for $k > 0$; for $k \leq 0$, (i) gives $|\mathcal{E}(f)(\mu^k u)| \leq C\mu^{k/2}$, and hence the required uniform geometric convergence follows. ∎

The scaling action of $\mathbb{R}_+^*$ on functions is defined by $(\vartheta(\lambda) f)(x) := f(\lambda^{-1} x)$. The next lemma describes the behavior of the scaling action in relation to the map $\mathcal{E}$.

Lemma 6.2. (i) *The Schwartz space $\mathcal{S}_0^{\mathrm{ev}}$ is globally invariant under the scaling action ϑ and with $\mu > 1$, the following equalities hold*

$$\mathcal{E} \circ \lambda^{-1/2} \vartheta(\lambda) = \vartheta(\lambda) \circ \mathcal{E}, \quad \vartheta(\lambda) \Sigma_\mu = \Sigma_\mu \vartheta(\lambda) \tag{6.3}$$

(ii) *The scaling action ϑ induces an action of the multiplicative group $C_\mu = \mathbb{R}_+^*/\mu^{\mathbb{Z}}$ on $\Sigma_\mu \mathcal{E}(\mathcal{S}_0^{\mathrm{ev}})$.*

(iii) *Let f be a function as in Lemma 6.1 that coincides near zero with a smooth even function, then $\Sigma_\mu \mathcal{E}(f)$ belongs to the closure of $\Sigma_\mu \mathcal{E}(\mathcal{S}_0^{\mathrm{ev}})$ in $L^2(C_\mu)$.*

Proof. The conditions defining the subspace $\mathcal{S}_0^{\mathrm{ev}} \subset \mathcal{S}(\mathbb{R})$ are invariant under the scaling action. One has

$$\mathcal{E}(\vartheta(\lambda)f)(u) = u^{1/2} \sum_{n>0} f(n\lambda^{-1}u) = \lambda^{1/2}\vartheta(\lambda)(\mathcal{E}(f))(u).$$

Moreover, one has $\vartheta(\lambda)\Sigma_\mu = \Sigma_\mu \vartheta(\lambda)$. Thus, since $\mathcal{S}_0^{\mathrm{ev}}$ is invariant under the scaling action, the same invariance holds for its image $\Sigma_\mu \mathcal{E}(\mathcal{S}_0^{\mathrm{ev}})$ on which the scaling action is now periodic of period μ. From this fact one derives an induced action of the multiplicative group $C_\mu = \mathbb{R}_+^*/\mu^{\mathbb{Z}}$. Let f be as in Lemma 6.1. Let $\varepsilon > 0$ and $\rho \in C_c^\infty(\mathbb{R}_+^*)$ have support in a small neighborhood of 1 and be such that, for the norm in $L^2(C_\mu)$,

$$\|\vartheta(\rho)\Sigma_\mu \mathcal{E}(f) - \Sigma_\mu \mathcal{E}(f)\| < \varepsilon.$$

By applying (6.3) for a $\widetilde{\rho} \in C_c^\infty(\mathbb{R}_+^*)$ with the same support as ρ, one has

$$\vartheta(\rho)\Sigma_\mu \mathcal{E}(f) = \Sigma_\mu \mathcal{E}(\vartheta(\widetilde{\rho})(f)).$$

Finally, the hypothesis on f show that the function $\vartheta(\widetilde{\rho})(f)$ belongs to $\mathcal{S}_0^{\mathrm{ev}}$. ∎

6.2. Zeros of zeta and ζ-cycles. We identify a circle of length $L = \log \mu > 0$ with the quotient space $C_\mu := \mathbb{R}_+^*/\mu^{\mathbb{Z}}$ viewed as a homogeneous space over the multiplicative group $\mathbb{R}_+^*$. This space is endowed with the measure d^*u associated to the Haar measure of the multiplicative group $\mathbb{R}_+^*$. One thus obtains a canonical bundle of $\mathbb{R}_+^*$-homogeneous spaces over the base $(0, \infty)$.

We keep the notations introduced in the previous part.

Definition 6.1. A *ζ-cycle* is a circle C of length $L = \log \mu$ such that the subspace $\Sigma_\mu \mathcal{E}(\mathcal{S}_0^{\mathrm{ev}})$ is not dense in the Hilbert space $L^2(C)$.

As for closed geodesics, the ζ-cycles are stable under finite covers.

Proposition 6.3. *Let C be a ζ-cycle of length $L = \log \mu$, then for any positive integer $n > 0$ the n-fold cover of C is a ζ-cycle.*

Proof. Let $\pi : C_n \to C$ be the n-fold cover of C. From the adjunction of the operation $\pi^* : L^2(C) \to L^2(C_n)$ with the operation of sum on the preimage of a point, it follows that if a vector $\xi \in L^2(C)$ belongs to the orthogonal to $\Sigma_\mu \mathcal{E}(\mathcal{S}_0^{\mathrm{ev}}) \subset L^2(C)$ with $\mu = \exp L$, then $\pi^*\xi$ is orthogonal to $\Sigma_{\mu^n} \mathcal{E}(\mathcal{S}_0^{\mathrm{ev}})$. ∎

We are now ready to state and prove our main result. The spectral realization of the zeros of the Riemann zeta function of [4] admits the following geometric variant

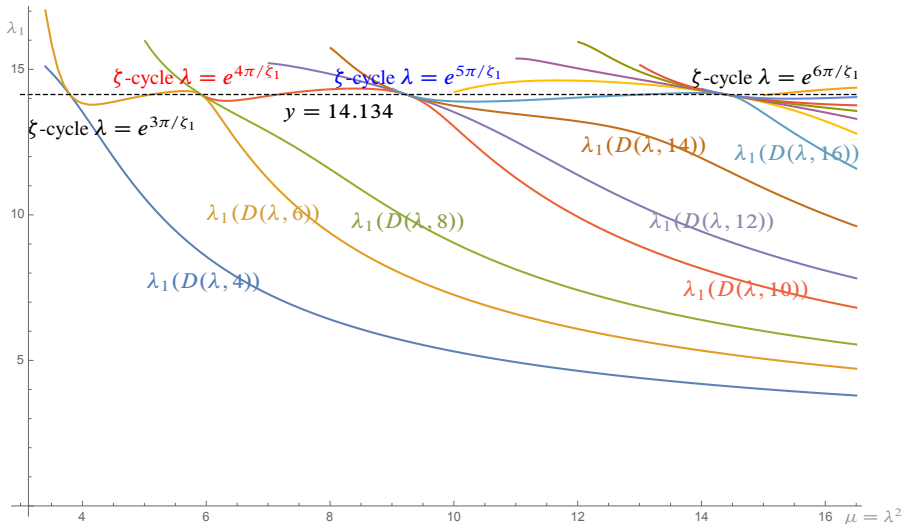

FIGURE 54
Example of ζ-cycles. They are shown here for the first non-zero eigenvalue $\lambda_1(D(\lambda, k))$. The graphs touch each other at the points $P(k) = (\exp(2\pi k/\zeta_1), \zeta_1)$.

Theorem 6.4. (i) *Let C be a ζ-cycle. Then the spectrum of the action of the multiplicative group $\mathbb{R}_+^*$ on the orthogonal complement of $\Sigma_\mu \mathcal{E}(\mathcal{S}_0^{\mathrm{ev}})$ in $L^2(C)$ is formed by imaginary parts of zeros of zeta on the critical line. Conversely:*

(ii) *Let $s > 0$ be such that $\zeta(\frac{1}{2} + is) = 0$, then any real circle C of length an integral multiple of $2\pi/s$ is a zeta cycle and its spectrum, for the action of $\mathbb{R}_+^*$ on $\Sigma_\mu \mathcal{E}(\mathcal{S}_0^{\mathrm{ev}}) \subset L^2(C)$, contains is.*

Proof. (i) The action of the multiplicative group $\mathbb{R}_+^*$ on the orthogonal of $\Sigma_\mu \mathcal{E}(\mathcal{S}_0^{\mathrm{ev}})$ in $L^2(C)$ is periodic and factors through the action of the multiplicative group $G = \mathbb{R}_+^*/\mu^{\mathbb{Z}}$. Since G is a compact abelian group the representation of G is a direct sum of unitary characters. Let χ be any such unitary character, then there then exists $s \in \mathbb{R}$ with $\mu^{is} = 1$, such that $\chi(u) = u^{is}$ for all $u \in G = \mathbb{R}_+^*/\mu^{\mathbb{Z}}$. The orthogonality property of an eigenvector with eigenvalue χ with respect to the subspace $\Sigma_\mu \mathcal{E}(\mathcal{S}_0^{\mathrm{ev}}) \subset L^2(C)$ implies the following vanishing

$$\int_G \chi(u) \Sigma_\mu \mathcal{E}(f)(u)\, d^*u = 0, \quad \forall f \in \mathcal{S}_0^{\mathrm{ev}}.$$

In turn, this implies the vanishing of the following integral

$$\int_{\mathbb{R}_+^*} u^{is} \mathcal{E}(f)(u)\, d^*u = 0, \quad \forall f \in \mathcal{S}_0^{\mathrm{ev}}.$$

Let, in particular,

$$f(x) := e^{-\pi x^2}\pi x^2(-2\pi x^2 + 3).$$

One easily checks that

$$\int_0^\infty f(x)\,dx = 0$$

and that $f \in \mathcal{S}_0^{\mathrm{ev}}$. Furthermore, one has

$$\int_{\mathbb{R}_+^*} u^{is} f(u)\,d^*u = \Big(\frac{1}{4} + s^2\Big)\pi^{-\frac{1}{4}-\frac{is}{2}}\Gamma\Big(\frac{1}{4} + \frac{is}{2}\Big)$$

and, as we shall prove in general in the following part for functions $f \in \mathcal{S}_0^{\mathrm{ev}}$, one also has

$$\int_{\mathbb{R}_+^*} u^{is}\mathcal{E}(f)(u)\,d^*u = \zeta\Big(\frac{1}{2} + is\Big)\int_{\mathbb{R}_+^*} u^{is} f(u)\,d^*u.$$

This fact entails that for the specific choice of f made above, one obtains the equality

$$\int_{\mathbb{R}_+^*} u^{is}\mathcal{E}(f)(u)\,d^*u = \Big(\frac{1}{4} + s^2\Big)\zeta_{\mathbb{Q}}\Big(\frac{1}{2} + is\Big),$$

where $\zeta_{\mathbb{Q}}$ denotes the complete zeta function. Thus one derives that $\frac{1}{2} + is$ is a zero of zeta.

(ii) Let $s > 0$ be such that $\zeta(\frac{1}{2} + is) = 0$ and let $L = 2\pi n/s$, with $n > 0$ a positive integer. To show that the circle C of length L is a zeta cycle, we first prove that

$$\int_{\mathbb{R}_+^*} u^{is}\mathcal{E}(f)(u)\,d^*u = 0, \quad \forall f \in \mathcal{S}_0^{\mathrm{ev}}.$$

Indeed, let $f \in \mathcal{S}_0^{\mathrm{ev}}$, then with w being the unitary identification $w(f)(x) = x^{1/2} f(x)$, the multiplicative Fourier transform $\mathbb{F}_\mu(w(f)) = \psi$:

$$\psi(z) = \int_{\mathbb{R}_+^*} f(u)u^{\frac{1}{2}-iz}\,d^*u$$

is holomorphic in the half plane $\Im(z) > -5/2$, since $f(u) = O(u^2)$ for $u \to 0$. For $n > 0$, one obtains

$$\int_{\mathbb{R}_+^*} u^{1/2} f(nu)u^{-iz}\,d^*u = n^{-1/2+iz}\int_{\mathbb{R}_+^*} v^{1/2} f(v)v^{-iz}\,d^*v$$

and for $\Im(z) > 1/2$, by applying the Fubini theorem, one derives

$$\int_{\mathbb{R}_+^*} \sum_n u^{1/2} f(nu)u^{-iz}d^*u = \Big(\sum_n n^{-1/2+iz}\Big)\int_{\mathbb{R}_+^*} v^{1/2} f(v)v^{-iz}\,d^*v,$$

so that for $z \in \mathbb{C}$ with $\Im(z) > 1/2$, one obtains

$$\int_{\mathbb{R}_+^*} \mathcal{E}(f)(u) u^{-iz}\, d^*u = \zeta\Big(\frac{1}{2} - iz\Big)\psi(z). \tag{6.4}$$

To justify the use of the Fubini theorem in proving (6.4), note that for $N > 1$ one derives from Lemma 6.1 the following estimate

$$\sum_{n\geq 1} |f(nu)| \leq C u^{-N} \sum_{n\geq 1} n^{-N} = C' u^{-N}, \quad \forall u > 1,$$

which shows that the series $\sum_{n\geq 1} |f(nu)|$ is of rapid decay for $u \to \infty$. For $u \to 0$ we use instead the rough estimate, due to the absolute integrability of f, of the form

$$\sum |f(nu)| = O(u^{-1}).$$

This ensures the validity of Fubini for $\Im(z) > 1/2$. Now, we know that $\zeta(\frac{1}{2} - iz)$ has a pole at $z = i/2$, but since $\psi(i/2) = 0$ this singularity does not affect the above product $\zeta(\frac{1}{2} - iz)\psi(z)$ which is thus holomorphic in the half plane $\Im(z) > -5/2$. By applying Lemma 6.1, we see that the function $\mathcal{E}(f)(u)$ is $O(u^{1/2})$ when $u \to 0$ and of rapid decay for $u \to \infty$. Thus,

$$\int_{\mathbb{R}_+^*} \mathcal{E}(f)(u) u^{-iz}\, d^*u$$

is holomorphic in the half-plane $\Im(z) > -1/2$. Therefore, one may conclude that (6.4) holds when $z \in \mathbb{R}$ and, if $\zeta(\frac{1}{2} + is) = 0$, one obtains

$$\int_{\mathbb{R}_+^*} \mathcal{E}(f)(u) u^{is}\, d^*u = 0, \quad \forall f \in \mathcal{S}_0^{\mathrm{ev}}.$$

At the beginning of this proof one has defined $L = 2\pi n/s$: let now $\mu = \exp L$ then one has $\mu^{is} = \exp(2\pi i n) = 1$. In this way the function $\chi(u) := u^{is}$ is well-defined on $C = \mathbb{R}_+^*/\mu^{\mathbb{Z}}$ and the following vanishing holds in $L^2(C)$

$$\langle \Sigma_\mu \mathcal{E}(f) \mid \chi \rangle = \int_G \chi(u) \Sigma_\mu \mathcal{E}(f)(u)\, d^*u = \int_{\mathbb{R}_+^*} \mathcal{E}(f)(u) u^{is}\, d^*u = 0, \quad \forall f \in \mathcal{S}_0^{\mathrm{ev}}.$$

This shows that C is a zeta-cycle and that its spectrum contains is. ∎

The above development provides us with a family of Hilbert spaces $\mathcal{H}(L) := \Sigma_\mu \mathcal{E}(\mathcal{S}_0^{\mathrm{ev}})^\perp \subset L^2(C)$ and, for each integer $n > 0$, maps $\pi_n^* : \mathcal{H}(L) \to \mathcal{H}(nL)$ which lift the action of $\mathbb{N}^\times$ on $(0, \infty)$. Moreover, we also have an action $\vartheta(\lambda)$ of $\mathbb{R}_+^*$ on $\mathcal{H}(L)$ and we have shown that the linear maps π_n^* are equivariant. Let Z be the set of imaginary parts of critical zeros of the Riemann zeta function, one finally deduces the following corollary.

Corollary 6.5.

$$\mathcal{H}(L) \neq \{0\} \iff \exists s \in Z,\ n \in \mathbb{Z}\ s.t.\ sL = 2\pi n. \tag{6.5}$$

Proof. Assume first that $sL = n$ with s and n positive. Then it follows from Theorem 6.4 (ii) that $\mathcal{H}(L) \neq \{0\}$ since the circle of length L is a zeta-cycle. Conversely, if $\mathcal{H}(L) \neq \{0\}$, then the circle C of length L is a zeta-cycle, and there exists by Theorem 6.4 (i), a positive $s \in Z$ and a non-zero vector $\xi \in \mathcal{H}(L)$ such that $\vartheta(\lambda)(\xi) = \lambda^{is}\xi$ for all $\lambda \in \mathbb{R}_+^*$. Since the action of $\mathbb{R}_+^*$ on $L^2(C)$ is periodic of period $\mu = \exp(L)$, we have $\mu^{is} = 1$ and this entails $sL \in 2\pi\mathbb{Z}$. ∎

7. Outlook

In this paper we have unveiled a new compelling relation between noncommutative geometry and the Riemann zeta function using the concept of spectral triple. The previous relations are:

- The BC system is a system of quantum statistical mechanics with spontaneous symmetry breaking which admits the Riemann zeta function as its partition function.
- The adele class space of $\mathbb{Q}$ is a noncommutative space, dual to the BC-system and directly related to the zeros of the L-functions with Grossencharacter [4].
- The quantized calculus is a key ingredient of the semi-local trace formula and it provides a source of positivity for the Weil quadratic form [6].

It turns out that the adele class space of $\mathbb{Q}$ in its topos-theoretic incarnation as the Scaling Site (the topos $\mathcal{S} = [0, \infty) \rtimes \mathbb{N}^\times$) is the natural parameter space for the circles of length L which play a critical role in the present paper. Proposition 6.3 gives the compatibility of ζ-cycles with the action of $\mathbb{N}^\times$ by multiplication on the parameter L. The action of $\mathbb{N}^\times$ coming from coverings turns $L^2(C)$ into a sheaf over the Scaling Site $\mathcal{S}$. The family of subspaces $\Sigma_\mu \mathcal{E}(\mathcal{S}_0) \subset L^2(C)$ generate a subsheaf of modules over the sheaf of smooth functions and one is then entitled to consider the cohomology of the quotient sheaf over $\mathcal{S}$. Endowed with the $\mathbb{R}_+^*$-equivariance this cohomology provides the spectral realization of the critical zeros of zeta, taking care, in particular, of eventual multiplicity. We shall discuss this fact in details in a forthcoming paper which, in particular, gives an application of the algebraic geometry over $\mathbb{S}$ developed in [5].

Finally, the stability of ζ-cycles under coverings is reminiscent of the behavior of closed geodesics in a Riemannian manifold, suggesting to look for a mysterious "cusp" whose closed geodesics would correspond to ζ-cycles.

Funding. The second author is partially supported by the Simons Foundation collaboration grant n. 691493.

References

[1] M. V. Berry, The Riemann–Siegel expansion for the zeta function: high orders and remainders. *Proc. Roy. Soc. London Ser. A* **450** (1995), no. 1939, 439–462. Zbl 0842.11030 MR 1349513

[2] E. Bombieri, The Riemann hypothesis. In *The millennium prize problems*, pp. 107–124, Clay Mathematics Institute, Cambridge, MA, 2006. Zbl 1194.11001 MR 2238277

[3] A. Connes, *Noncommutative geometry*. Academic Press, San Diego, CA, 1994. Zbl 0818.46076 MR 1303779

[4] — Trace formula in noncommutative geometry and the zeros of the Riemann zeta function. *Selecta Math. (N.S.)* **5** (1999), no. 1, 29–106. Zbl 0945.11015 MR 1694895

[5] A. Connes and C. Consani, On absolute algebraic geometry the affine case. *Adv. Math.* **390** (2021), Paper No. 107909. Zbl 1478.14047 MR 4291468

[6] — Weil positivity and trace formula the archimedean place. *Selecta Math. (N.S.)* **27** (2021), no. 4, Paper No. 77. Zbl 1480.46084 MR 4292787

[7] S. J. Patterson, *An introduction to the theory of the Riemann zeta-function*. Cambridge Stud. Adv. Math. 14, Cambridge University Press, Cambridge, 1988. Zbl 0831.11045 MR 933558

[8] W. Rudin, *Real and complex analysis*. Third edn., McGraw-Hill Book Co., New York, 1987. Zbl 0925.00005 MR 924157

[9] K. Schmüdgen, *Unbounded self-adjoint operators on Hilbert space*. Grad. Texts in Math. 265, Springer, Dordrecht, 2012. Zbl 1257.47001 MR 2953553

[10] B. Simon, Lower semicontinuity of positive quadratic forms. *Proc. Roy. Soc. Edinburgh Sect. A* **79** (1977/78), no. 3–4, 267–273. Zbl 0442.47017 MR 512713

[11] D. Slepian, Some asymptotic expansions for prolate spheroidal wave functions. *J. Math. and Phys.* **44** (1965), 99–140. Zbl 0128.29601 MR 179392

[12] — Some comments on Fourier analysis, uncertainty and modeling. *SIAM Rev.* **25** (1983), no. 3, 379–393. Zbl 0571.94004 MR 710468

[13] D. Slepian and H. O. Pollak, Prolate spheroidal wave functions, Fourier analysis and uncertainty. I. *Bell System Tech. J.* **40** (1961), 43–63. Zbl 0184.08601 MR 140732

[14] H. Yoshida, On Hermitian forms attached to zeta functions. In *Zeta functions in geometry (Tokyo, 1990)*, pp. 281–325, Adv. Stud. Pure Math. 21, Kinokuniya, Tokyo, 1992. Zbl 0817.11041 MR 1210794

(Reçu le 3 juin 2021)

Alain Connes, Collège de France, 3 rue d'Ulm, Paris 75005; and IHES, 35 route de Chartres, 91440 Bures-sur-Yvette, France; *e-mail:* alain@connes.org

Caterina Consani, Department of Mathematics, Johns Hopkins University, Baltimore 21218, USA; *e-mail:* cconsan1@jhu.edu